TECHNICAL REPORT R-20

TIRE-TO-SURFACE FRICTION-COEFFICIENT MEASUREMENTS WITH A C-123B AIRPLANE ON VARIOUS RUNWAY SURFACES

By RICHARD H. SAWYER and JOSEPH J. KOLNICK

Langley Research Center
Langley Field, Va.

TECHNICAL REPORT R-20

TIRE-TO-SURFACE FRICTION-COEFFICIENT MEASUREMENTS WITH A C-123B AIRPLANE ON VARIOUS RUNWAY SURFACES

By Richard H. Sawyer and Joseph J. Kolnick

SUMMARY

An investigation was conducted to obtain information on the tire-to-surface friction coefficients available in aircraft braking during the landing run. The tests were made with a C-123B airplane on both wet and dry concrete and bituminous pavements and on snow-covered and ice surfaces at speeds from 12 to 115 knots. Measurements were made of the maximum (incipient skidding) friction coefficient, the full-skidding (locked wheel) friction coefficient, and the wheel slip ratio during braking.

The mean value of the maximum friction coefficient on both dry portland-cement concrete and dry bituminous pavements was about 0.8, with no effect of speed or load evident over the ranges investigated. For snow-covered surfaces, the mean value of maximum friction coefficient varied from 0.25 to 0.37; the lower values were apparently associated with icy subsurfaces under the snow and the higher values with bare pavement subsurfaces. Over the ranges of the investigation, no effects of speed or surface temperature (3° F to 32° F) on the maximum friction coefficient were evident. On an ice surface, the mean value of the maximum friction coefficient was 0.18 at surface temperatures of both 19° F and 32° F, with no apparent dependence on speed. For wet portland-cement concrete and bituminous pavement surfaces, values of maximum friction coefficient varied from 0.04 to more than 0.80. The variations in maximum friction coefficient were believed to be associated primarily with variations in depths of water along the runway. The extremely low values were ascribed to planing of the tire on a film of water.

Full-skid (that is, locked wheel) friction coefficients on the dry, snow-covered, and ice surfaces were found to decrease with decrease in speed as the skid progressed, reaching values between about 0.1 and 0.2. On the wet surfaces, the full-skid friction coefficient was near zero at the higher speeds and increased to about 0.3 as the skid progressed to lower speeds.

INTRODUCTION

The coefficient of friction which can be developed between an airplane's tires and a runway surface is, in many cases, a primary factor in determining whether the airplane can make a safe stop in landing on a given runway. Therefore, an adequate understanding of tire friction characteristics under all the conditions likely to be encountered in airplane operation is important to a number of groups: airplane designers in assessing the utilization potential of their designs, regulatory agencies in formulating rules for safe operations, operation groups in meeting their responsibilities for safe, economical, and on-time flight operations, and others.

Considerable information on tire-to-surface friction coefficients for road-vehicle applications has been obtained with a variety of road surface conditions. These results, however, were obtained with automobile tires at relatively low speeds (generally less than 40 knots) and there is considerable question as to the applicability of these results at the higher speeds, wheel loads, and tire inflation pressures characteristic of modern airplane operations. Moreover, most of the automobile-tire results were obtained with the full-skid or locked-wheel condition, whereas for airplane operations, particularly with the increasing use of automatic braking devices, it appears that the maximum value of friction coefficient developed with the wheels in the incipient-skidding condition is more pertinent. A very limited amount of information has been obtained for the incipient-skidding condition with airplane tires on wet and dry surfaces from measurements of spin-up loads in actual or simulated landing impacts (refs. 1 to 4) and from deceleration measurements in braked landings of an airplane equipped with an automatic braking system (British Ministry of Supply paper of limited distribution by H. J. Keyes). Other measurements have been made for the full-skid condition with airplane tires on a dry surface (ref. 5) and with a small low-pressure tire at high speeds (up to about 90 knots) on wet surfaces (ref. 6).

The present investigation was undertaken to provide information on tire friction coefficients more directly applicable to the airplane braking problem. Measurements were obtained in actual landing runs of a C-123B airplane. Particular attention was given to adverse surface conditions including wet, icy, and snow-covered runways. Results deal primarily with the incipient-skidding condition, although some data are presented for the full-skid condition. Information is also given on the variation of friction coefficient with slip ratio and on the slip ratio at which incipient skidding or maximum friction occurs. The smooth-contour tires used in the investigation were 48 inches in diameter, had a rib tread, and were inflated to a pressure of 65 pounds per square inch.

SYMBOLS

A_g	gross footprint area of tire, sq in.
A_n	net footprint area of tire, sq in.
b	width of tire-ground contact area (footprint), in.
F_h	horizontal force, lb
F_v	vertical force, lb
h	half-length of tire-ground contact area (footprint), in.
r_e	wheel rolling radius, 2.0 ft
s	slip ratio, $(\omega-\omega_b)/\omega$
$s_{max\ \mu}$	slip ratio at μ_{max}
T_B	brake torque, in-lb
V	airplane forward ground speed, knots
δ	vertical tire deflection, in.
μ	tire-to-surface coefficient of friction during braking, F_h/F_v
ω	wheel angular velocity for unbraked rolling, radians/sec
ω_b	wheel angular velocity for braked rolling, radians/sec

Subscripts:

a	axle
max	maximum
$full\ skid$	fully skidding wheel (that is, locked wheel)

DESCRIPTION OF APPARATUS

AIRPLANE

The C-123B airplane used in the investigation (fig. 1) was an assault-type troop carrier having a gross weight of about 45,000 pounds for these tests. Two features of this airplane, in particular, led to its selection as the test vehicle. One of these was the landing-gear structure, which met the requirements for a suitable strain-gage installation to measure the forces acting on the tires. The other feature was the mechanical-hydraulic antiskid braking system which could provide frequent cycling of the brake action and thereby produce the desired traverses of wheel slip ratio through the incipient-skidding or maximum-friction condition. In addition, the reversible propellers on this airplane insured that it could be stopped safely when operating on slippery surfaces.

INSTRUMENTATION

Strain gages were mounted on each of the main gear axles between the brake flange and the lower strut. (See fig. 2.) The gages were arranged to measure shear and bending-moment stresses in both the horizontal and vertical planes through the axle and the torsional stresses produced by brake torque. Linear strain-gage-type accelerometers were located on brackets attached to each brake flange to determine the horizontal and vertical inertia forces of the part of the gear between the ground-contact area of the tire and the axle strain-gage location.

The angular velocity of each wheel was measured by means of a pair of strain-gage accelerometers diametrically mounted on a plate attached to the outer face of the wheel (fig. 3). The accelerometers were mounted so as to measure radial acceleration and were coupled electrically so as to cancel linear accelerations. Since the

FIGURE 1. C-123B airplane used in the investigation.

radius was fixed, the output was proportional to the square of the angular velocity. The strain-gage and accelerometer outputs were all recorded on a photographically recording oscillograph.

The vertical and horizontal components of the acceleration of the center of gravity of the airplane were measured by means of a photographically recording, vane-type, air-damped two-component accelerometer.

TIRES

The main-gear tires used on the airplane were type III, 17.00-20, 16-ply rating and had a rib tread. The tires were operated at an inflation pressure of 65 pounds per square inch for all the tests, the recommended pressure for the static load carried on the main gear. The shape of the tire contact area for several loads is indicated in figure 4 by the outlines of footprint impressions made on cardboard backed by a concrete surface. The corresponding vertical tire deflections, gross and net footprint areas, and footprint length and width are also given. Each load for the footprints was applied rapidly and was removed before the next loading. This type of loading gives somewhat smaller tire deflections than a cumulative type of loading. Some of the chemical and physical properties of the tread material used in these tires are given in the following table:

Composition, percent:	
Rubber (natural)	57. 55
Carbon black	30. 16
Acetone extract	6. 53
Ash	2. 50
Zinc oxide	1. 63
Total sulfur	1. 63
Curing process:	
Type	McNeil watchcase press
Free sulfur (tread), percent	0. 10
Specific gravity	1. 124
Shore durometer hardness	60
Tensile strength, lb/sq in.:	
At 78° F	4, 000
At 120° F	3, 500
At 160° F	3, 000
At 200° F	2, 800
Goodyear ring abrasion, cm³ loss in 20 min	7. 50

SURFACES

Wet and dry portland-cement concrete and bituminous paved runways were used in the tests. All the wet runways tested were naturally wet from various amounts of rainfall. Several runways covered with snow deposits of various depths,

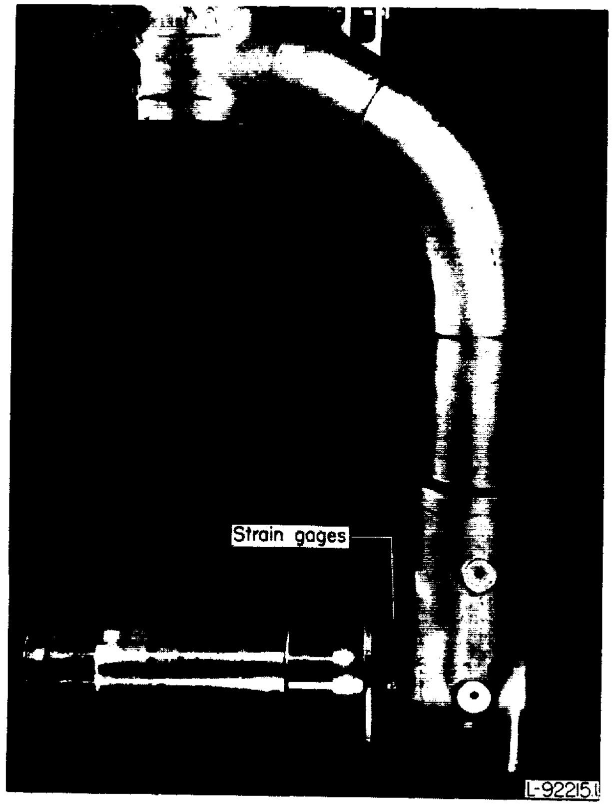

FIGURE 2. Main-gear lower strut and axle of C-123B airplane with strain gages installed.

ages, and degrees of wetness, hardness, and treatment were investigated. An ice runway was constructed by plowing the snow from the surface of a frozen lake, and another snow-covered runway was prepared alongside by removing only part of the snow from the lake surface. Detailed information on each of the runways is listed in table I.

A specially constructed camera was used in an attempt to obtain a measure of the texture of the runway surfaces. This camera was arranged to photograph at full scale the shadow of a line projected on the surface at an angle of 45° from the vertical. The lateral deviations of the shadow as photographed perpendicular to the surface thus show roughly the shape and height of the surface irregularities. Photographs of some of the runway surfaces made with the roughness camera are given in figure 5. The locations of fine and coarse line shadows for the roughness photographs are indicated on figure 5(a). In some instances it is very difficult to see the line shadows in the reproduced photograph.

TEST PROCEDURE

The results were obtained during the braked portion of the landing run. The pilot applied maximum pedal pressure in braking as soon as the nose wheel could be lowered after touchdown. This maximum braking effort provided brake torque which, in most instances, exceeded the maximum torque available from the frictional force between the tire and surface, and thus tended to lock the wheels. Actual locking of the wheels was prevented by the antiskid devices which fully released the brake pressure on command from the rapid angular deceleration of the wheel which occurred after the maximum frictional force was exceeded. The wheel which had been slowed down in angular velocity under the action of the braking was then allowed to spin up to free-rolling speed before the antiskid device allowed brake pressure to be reapplied. The overall action of the antiskid device resulted in a cyclic on-off action of the brakes. The wheel was thus cycled from free-rolling speed to an angular velocity less than that required to develop the maximum friction force. Consequently, whenever the applied braking torque exceeded the friction capabilities of the surface, the antiskid action provided a cyclic variation of the friction force from zero to beyond the maximum value. The antiskid device operated at about 2 cycles per second, and thus maximum friction values at a rate of about 2 per second were obtained during the braked portion of the landing run.

In some instances the flap deflections were varied during the landing run in order to increase the accuracy and amount of data obtained. Flap-up positions were used at high speeds to increase the loads on the main gear in order to promote better accuracy by making the measured loads large in comparison with the accuracy of measurement. Flap-down positions were used at low speeds to decrease the loads on the gear when a combination of high-friction characteristics of the surface and high load resulted in an available torque on the wheel from the friction force which tended to exceed the brake torque capabilities. Where feasible, downwind landings were made in order to increase the range of ground speeds. Ground speeds ranging from 12 knots to 115 knots were covered in the tests. In most instances, two or more landings were made on each surface.

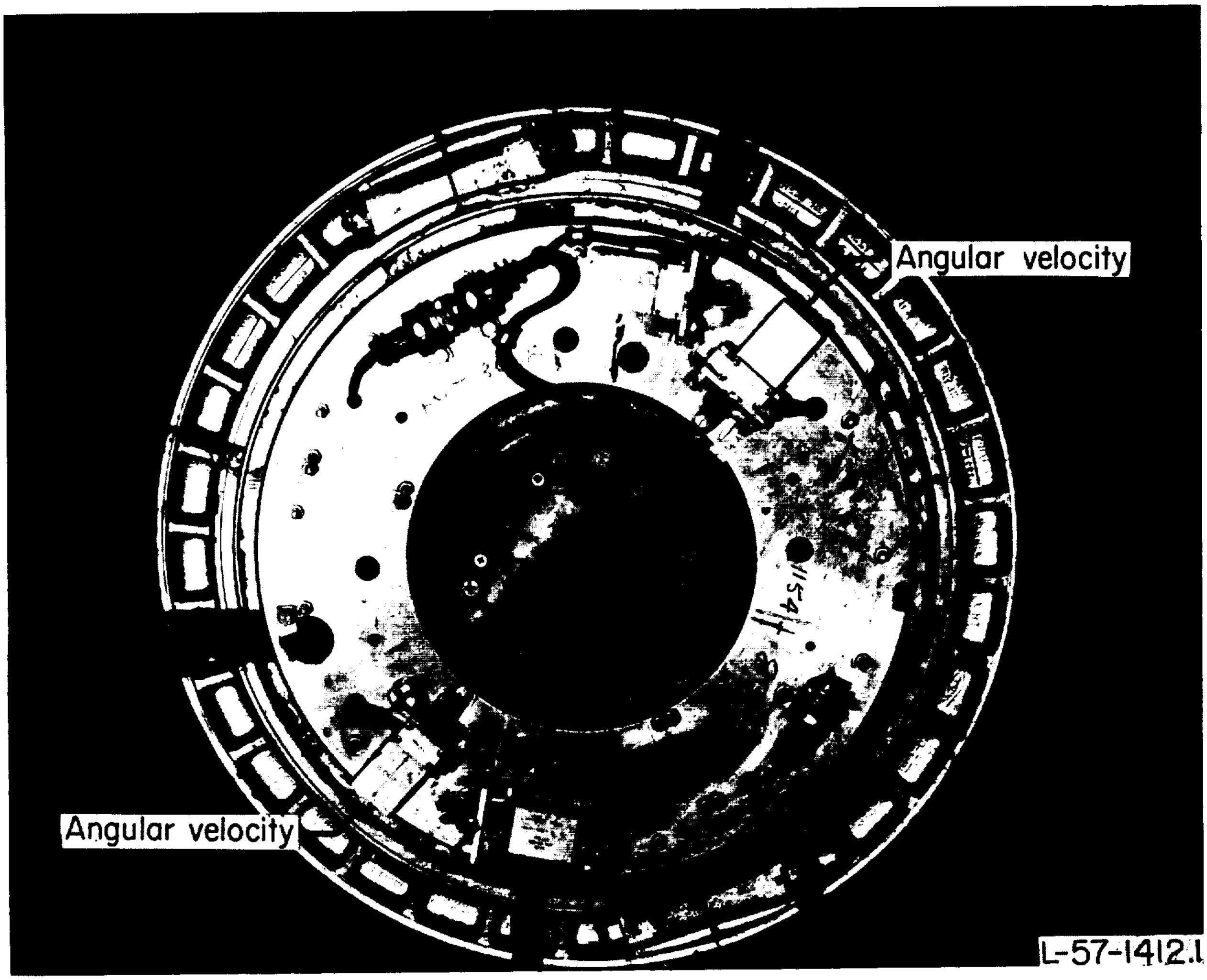

FIGURE 3. Main-gear wheel of C-123B airplane, showing arrangement of accelerometers used to measure angular velocity of the wheel.

As soon as possible after the tests were made, photographs of the surface roughness were made with the roughness camera. For the snow-covered surfaces, the depth of the snow and the subsurface conditions were noted. Also, the snow was classified by means of the simplified field classification system (prepared by the Snow, Ice and Permafrost Research Establishment) given in reference 7. Table II presents a copy of this system. Air and surface temperatures were obtained from measurements with both mercury-bulb and thermocouple thermometers as well as from airport weather-station data. For the tests made on the frozen lake, weather data were obtained by means of a portable automatic recording weather station (ref. 8). Observations of amount and rate of rainfall were obtained from airport weather-station data. Test conditions not presented in the figures showing the results (figs. 6 to 14) are listed in table I.

DATA REDUCTION

For each main gear, the axle strain-gage measurements were used to calculate the vertical and drag forces on the axle. The relationship between the strain-gage responses and the applied loads was determined by calibration loadings of each gear in the combined load testing machine of the Langley structures research laboratory (ref. 9). The combined loading calibrations resulted in relationships of the following form for the vertical and horizontal axle forces:

$$F_{v,h} = C_{v,1}d_{s,v} + C_{v,2}d_{m,v} + C_{v,3}d_{s,h} + C_{v,4}d_{m,h} + C_{v,5}d_t$$

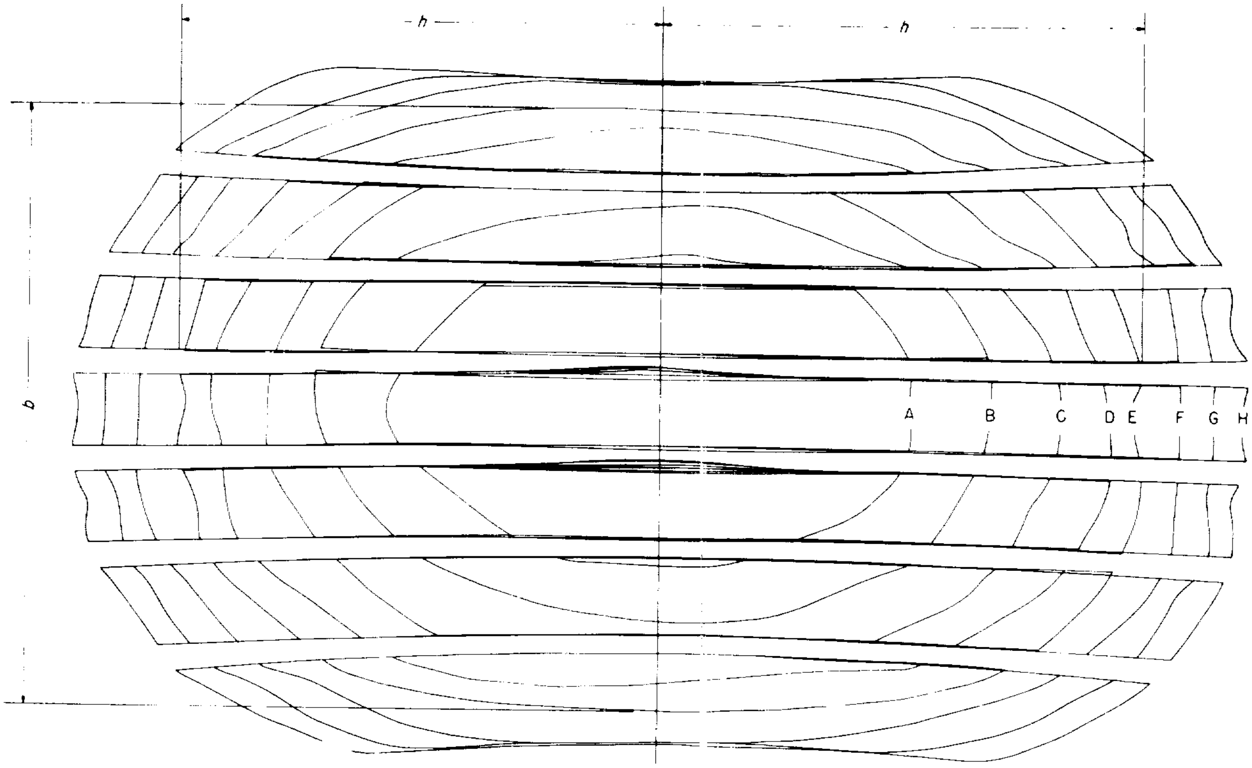

Footprint	F_v, lb	δ, in.	A_g, sq in.	A_n, sq in.	$2h$, in.	b, in.
A	5, 000	1. 21	48. 8	36. 9	10. 1	6. 0
B	7, 500	1. 81	83. 9	64. 9	13. 0	8. 0
C	9, 800	2. 33	119. 7	96. 1	15. 3	9. 2
D	12, 200	2. 83	153. 6	118. 1	17. 4	10. 8
E	14, 300	3. 27	184. 1	144. 3	18. 5	11. 6
F	16, 600	3. 72	219. 9	177. 4	20. 1	12. 7
G	18, 800	4. 13	243. 5	196. 4	21. 4	12. 8
H	20, 900	4. 51	265. 1	214. 1	22. 6	12. 8

FIGURE 4. Tire footprint diagrams and tire and footprint properties for type III, 17.00-20, 16-ply-rating rib-tread tires used in the investigation. Inflation pressure, 65 lb/sq in.

$$F_{h,a}=C_{h,1}d_{s,v}+C_{h,2}d_{m,v}+C_{h,3}d_{s,h}+C_{h,4}d_{m,h}+C_{h,5}d_t$$

where

$C_{v,1}, C_{v,2} \ldots$, $C_{h,1}, C_{h,2} \ldots$ constants determined from calibration loadings
$d_{s,v}$ output of vertical shear bridge
$d_{m,v}$ output of vertical moment bridge
$d_{s,h}$ output of horizontal shear bridge
$d_{m,h}$ output of horizontal moment bridge
d_t output of torque bridge

The existence of vertical gage terms in the horizontal equation and vice versa is the result of interaction effects as well as misalinement of gages.

The ground-reaction forces, both vertical and drag were obtained by adding inertia corrections to the axle forces. The inertia term was the product of the mass of the gear between the ground-contact area of the tire and the axle strain-gage location and the vertical or horizontal acceleration of this mass.

The ground speed was obtained by using the relationship $V=0.592\omega r_e$. The slip ratio was determined from the relationship $s=(\omega-\omega_b)/\omega$. The value of the free-rolling wheel speed ω during each braking cycle was determined by assuming that ω decreased linearly with time.

TABLE I
TEST SURFACES AND TEST CONDITIONS

Runway	Location	Runway number	Surface description	Test conditions
A	Langley AFB, Langley Field, Va.	7–25	Portland-cement concrete. Runway ends blackened with rubber deposits. For wet tests, surface wet enough so that tires threw a spray of water.	(a) Dry surface, air temperature 58° to 64° F. (b) Wet surface, air temperature 67° F.
B	Norfolk Municipal Airport, Norfolk, Va.	4–22	Dry bituminous pavement aggregate appears to be mixed crushed stone, mostly small size. Surface 15 or 16 years old.	Air temperature 71° F.
C	Byrd Airport, Richmond, Va.	2–20	Dry bituminous pavement part of surface relatively smooth texture and part rather rough texture. Aggregate appears to be a fine crushed rock.	Air temperature 77° F. Surface temperature 68° F.
D	Moisant International Airport, New Orleans, La.	10–28	Bituminous pavement surface texture uniformly smooth with only fine aggregate content. For landing made during heavy thundershowers, surface appeared covered with sheet of water ¼ inch to ½ inch deep.	(a) Dry surface, air temperature 81° F. (b) Wet surface, air temperature 66° F.
E	Loring AFB, Limestone, Maine.	1–19	Portland-cement concrete covered with old scraped snow that had been partially melted and refrozen. Ice coverage about 20 percent. One-fourth inch to ½ inch new, soft, moist snow on top.	Air temperature from 12° to 19° F.
F	Millinocket Airport, Millinocket, Maine.	11–29	Bituminous pavement covered by ¼ to ½ inch of new moist snow hard packed by recent ploughing.	Air temperature 16° to 17° F. Surface temperature 18° F. Tire broke through to subsurface frequently.
G	Millinocket Airport, Millinocket, Maine.	16–34	Ice-spotted bituminous pavement covered by 5 to 6 inches of new, soft, dry snow with 1/16-inch-thick crust.	Air temperature 16° to 17° F. Surface temperature 18° F. Tire broke through to subsurface frequently.
H	Bemidji Airport, Bemidji, Minn.	13–31	Bituminous pavement almost completely covered by icy packed snow subsurface under complete coverage of 1 to 2 inches of new, soft, dry snow.	Air temperature −5° to −2° F. Surface temperature 3° F. Tire broke through to subsurface.
I	Bemidji Airport, Bemidji, Minn.	13–31	Bituminous pavement almost completely covered by icy packed snow subsurface under complete coverage of 1 to 4 inches of new, soft, moist snow.	Air temperature 36° F. Surface temperature 32° F. Tire broke through to subsurface and occasionally to pavement.
J	Bemidji Lake, Bemidji, Minn.	14–32	Frozen lake surface covered by 5 inches old, soft-to-hard, moist-to-wet snow left when top 7-inch layer removed by ploughing.	Air temperature 32° F. Surface temperature 32° F.
K	Bemidji Lake, Bemidji, Minn.	14–32	Frozen lake surface covered by 5 inches old, hard, dry snow subsurface left by previous ploughing operation under 1 to 3 inches new, soft, dry snow.	Air temperature −2° F. Surface temperature 19° F.

TABLE I.—Concluded

TEST SURFACES AND TEST CONDITIONS

Runway	Location	Runway number	Surface description	Test conditions
L	Bemidji Lake, Bemidji, Minn.	14–32	Frozen lake surface. Thin, patchy snow residue left on ice from ploughing operation.	(a) Air temperature 30° F., surface temperature 32° F. (b) Air temperature 2° F., surface temperature 19° F.
M	Patrick Henry Airport, Newport News, Va.	6–24	Wet portland-cement concrete. Surface thoroughly wet by 2-hour period of light drizzle to light rain conditions. Tires threw spray of water. Deep puddles noted at runway intersections.	Air temperature 65° F.
N	Naval Air Station, Norfolk, Va.	10–28	Wet bituminous pavement. Asphalt concrete with granite chip aggregate. Surface 5 years old. Surface wet from previous rain and dotted with puddles.	Air temperature 60° F.

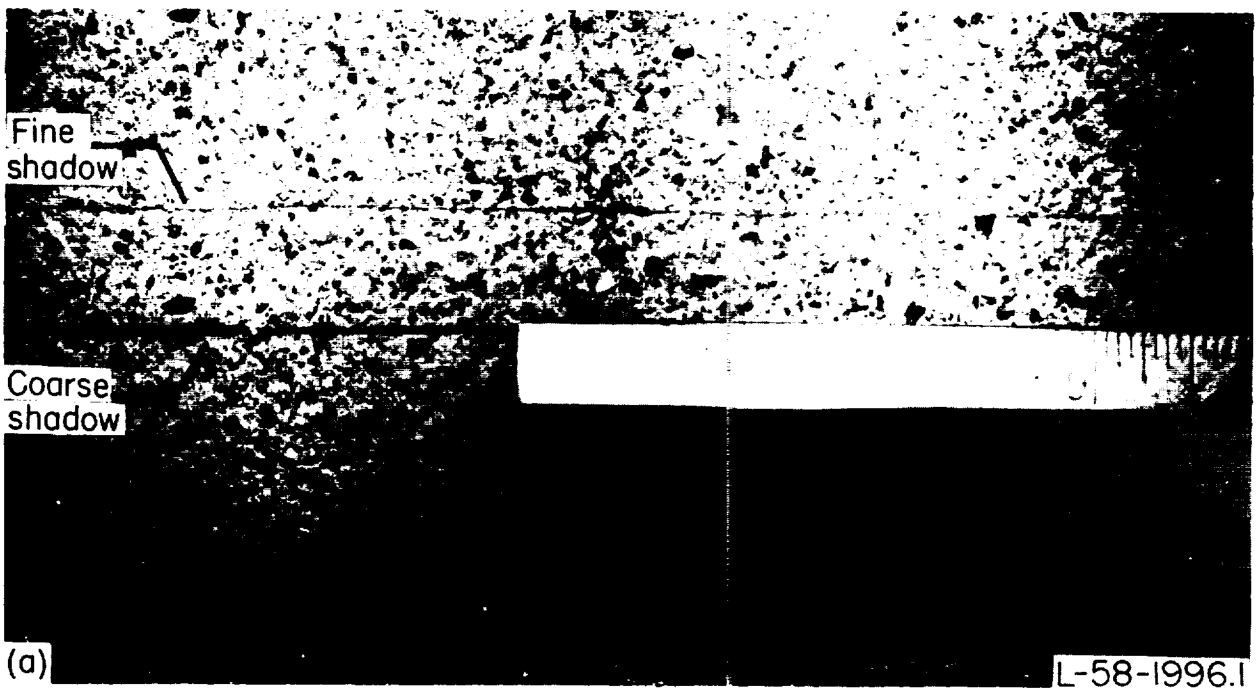

(a) Runway A, east end.

FIGURE 5.—Some of the runway surfaces on which tire-to-surface friction coefficients were measured during braking of the C-123B airplane.

(b) Runway A, west end.

FIGURE 5.—Continued.

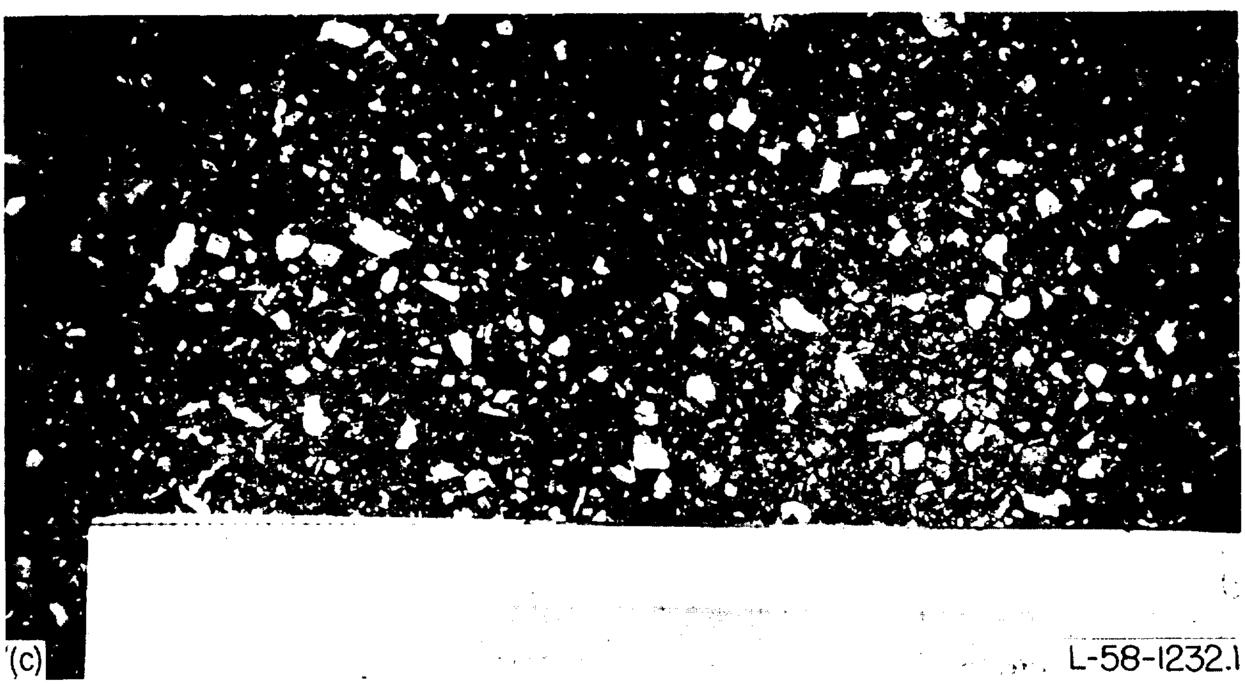

(c) Runway B, dense graded.

FIGURE 5.—Continued.

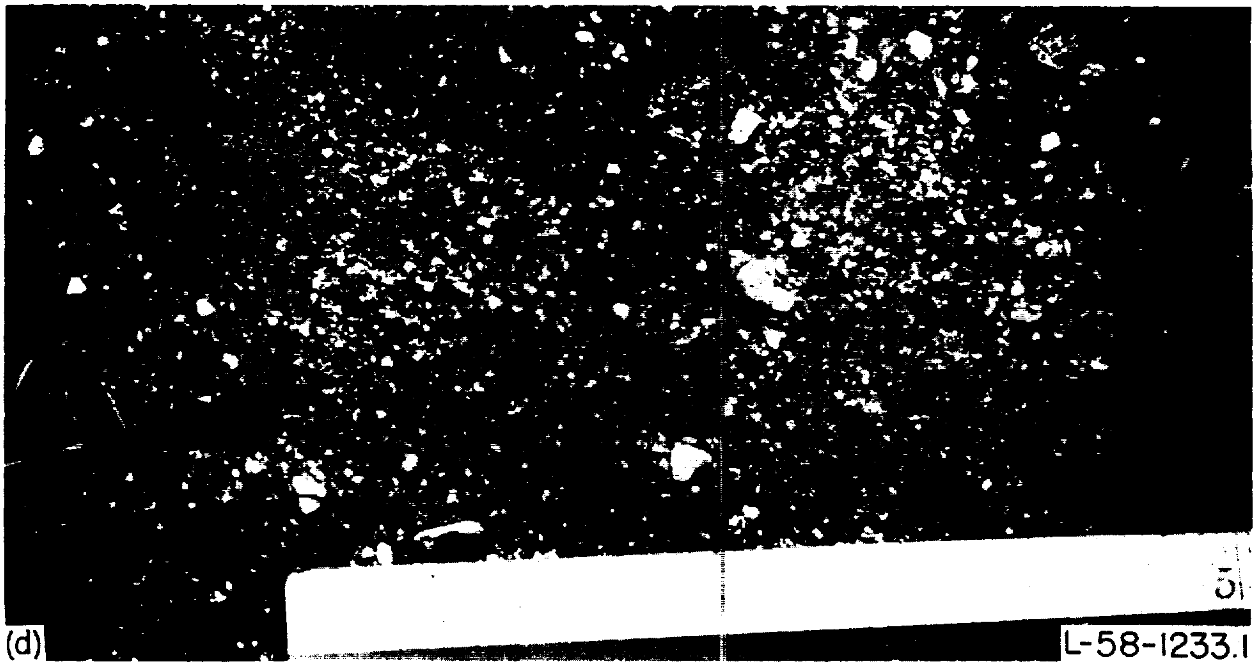

(d) Runway B, open graded.

FIGURE 5. Continued.

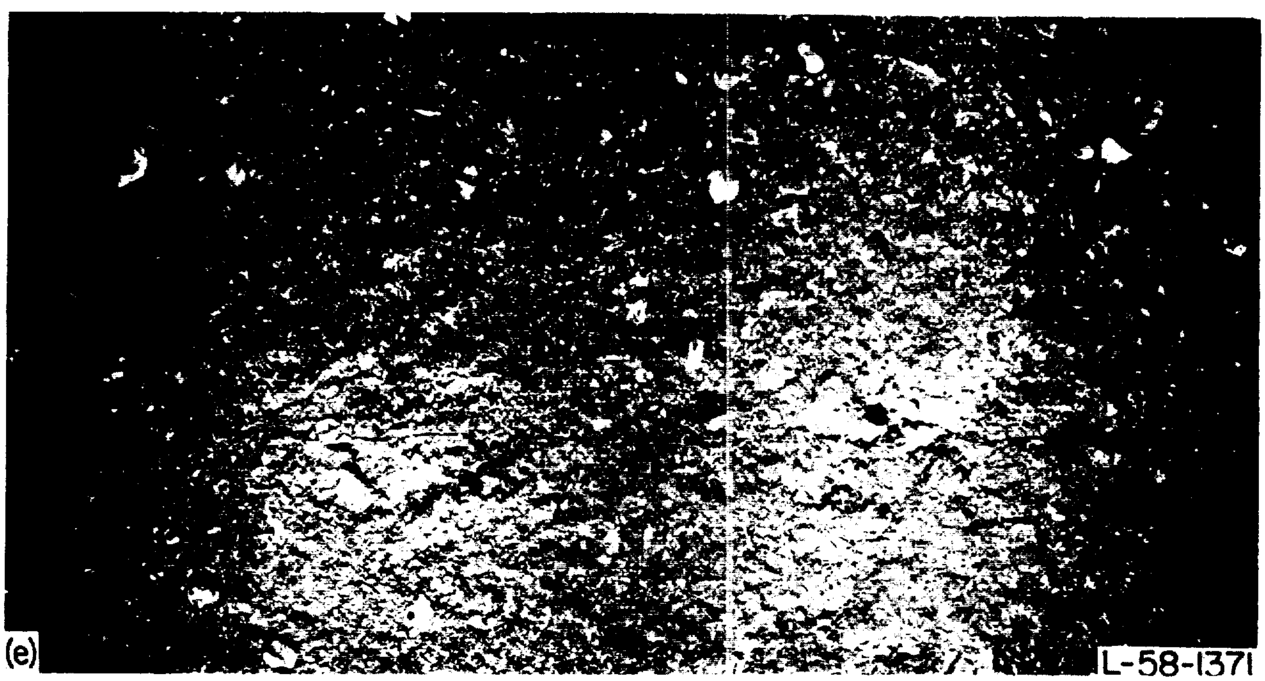

(e) Runway C, smooth texture.

FIGURE 5. Continued.

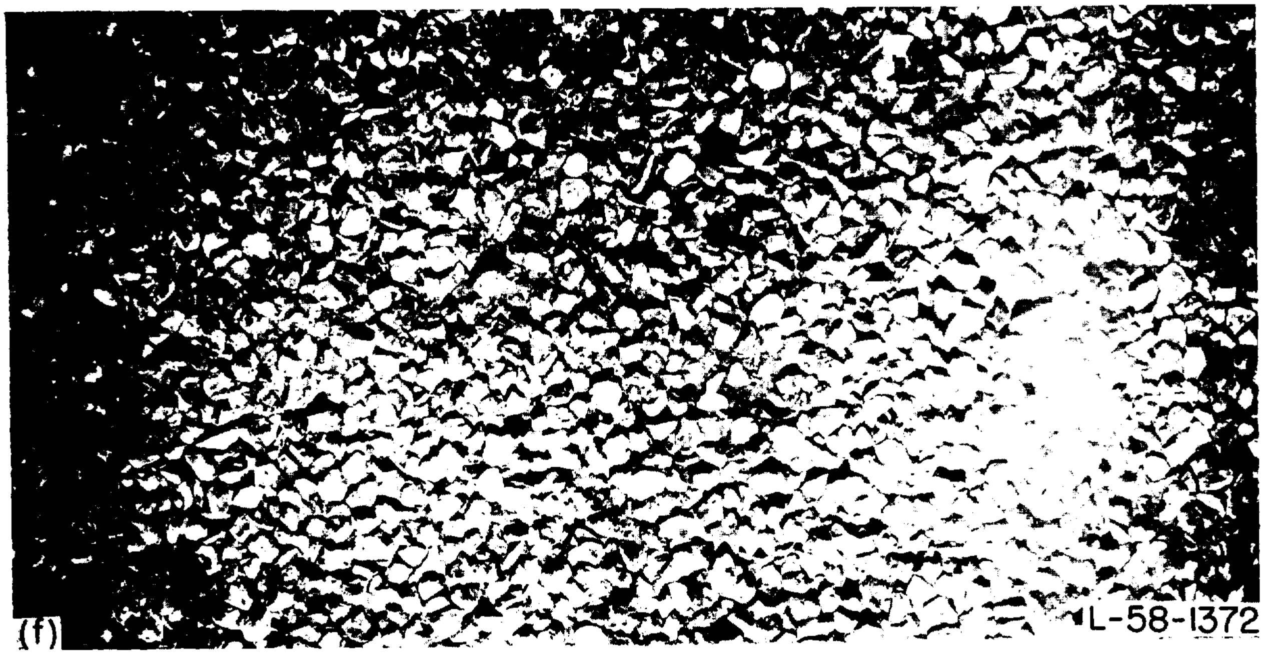

(f) Runway C, rough texture.

FIGURE 5. Continued.

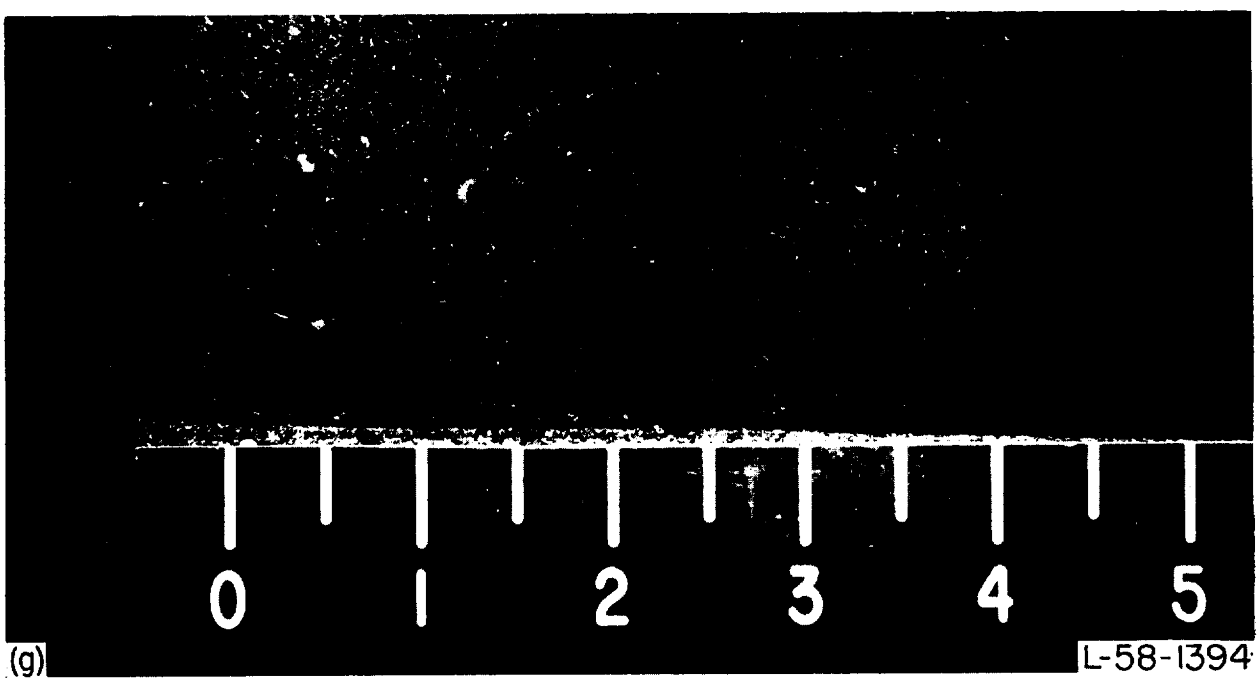

(g) Runway D.

FIGURE 5.—Continued.

(h) Runway I, breakthrough to pavement.

FIGURE 5. Continued.

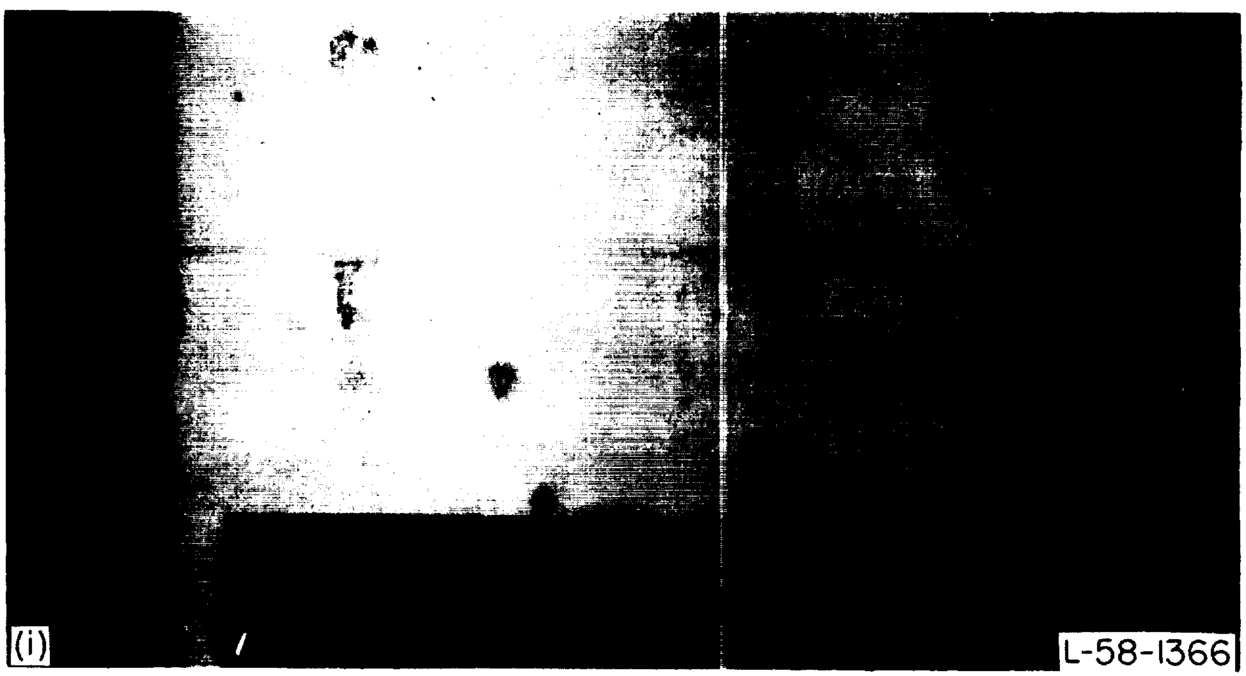

(i) Runway I, breakthrough to packed-snow subsurface.

FIGURE 5. Continued.

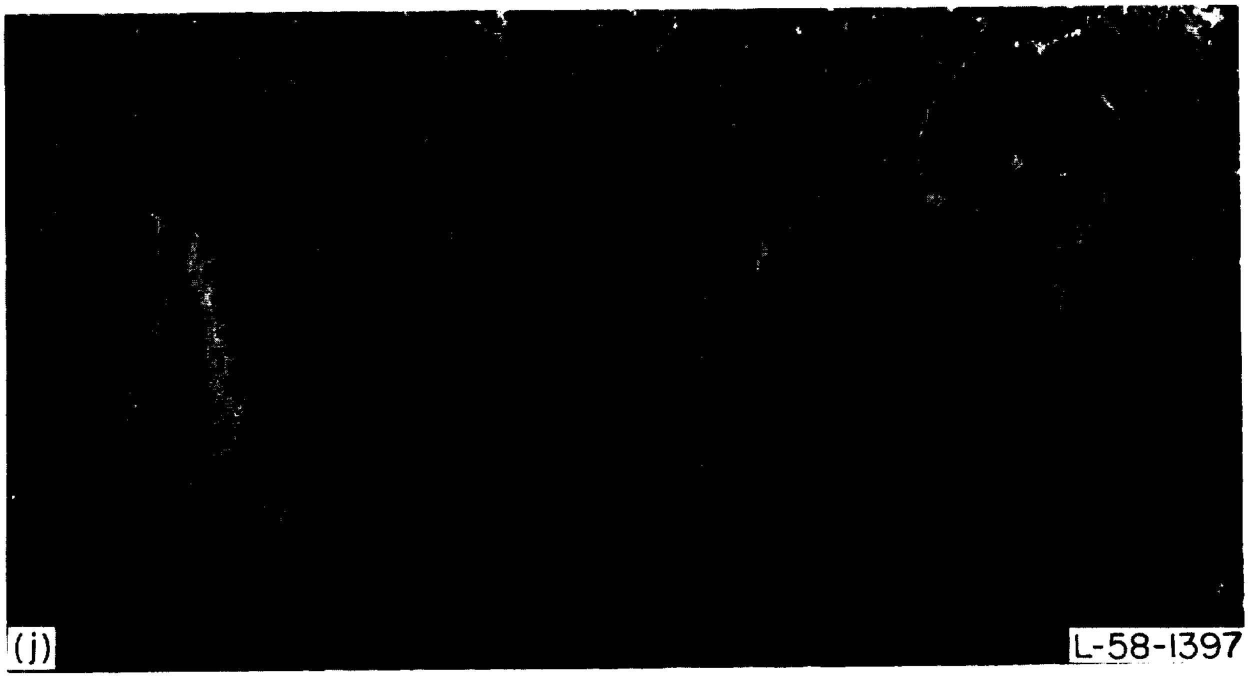

(j) Runway L.

FIGURE 5.—Continued.

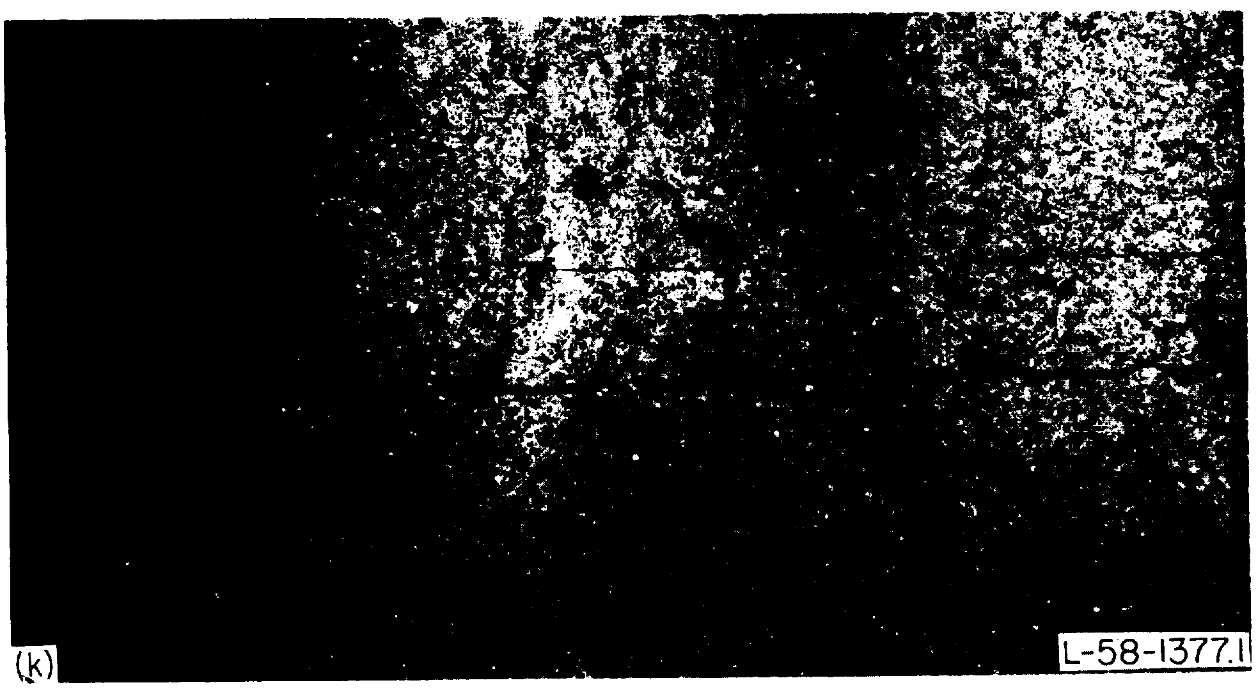

(k) Runway M, no deposits.

FIGURE 5.—Continued.

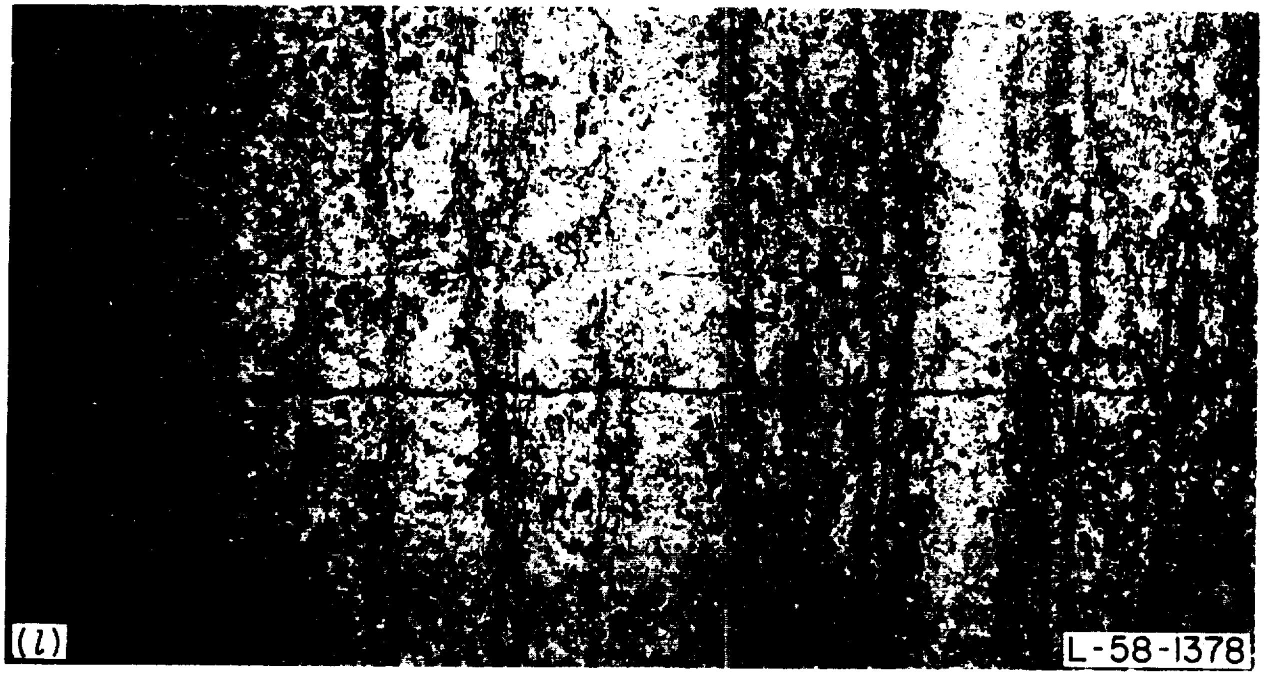

(l) Runway M, rubber deposits.

FIGURE 5. Continued.

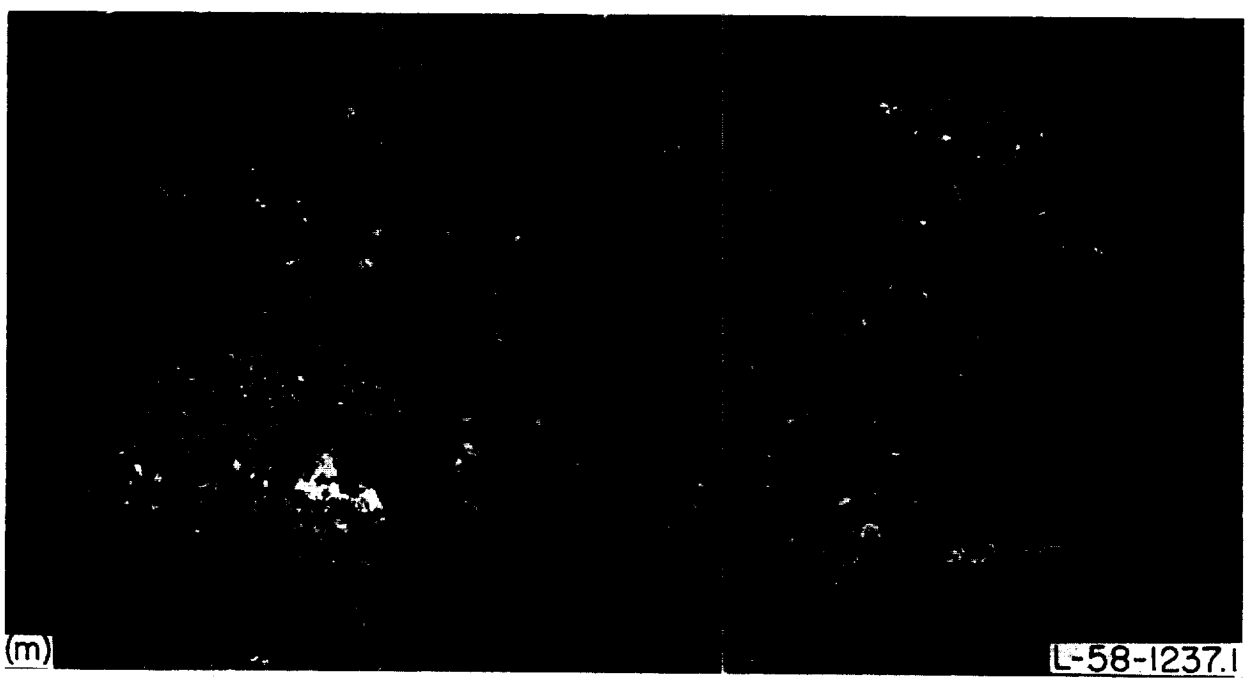

(m) Runway N.

FIGURE 5. Concluded.

TABLE II

SIMPLIFIED FIELD CLASSIFICATION OF NATURAL SNOW TYPES FOR ENGINEERING PURPOSES

Grain Nature
New snow (original crystal forms such as stars, plates, prisms, needles, and graupel granules are recognizable)
Old snow, granular, fine-grained (mean diameter is less than approximately 2 mm like table salt)
Old snow, granular, coarse-grained (mean diameter is larger than approximately 2 mm like coarse sand)
Depth hoar (cup-shaped crystals 3 to 10 mm diameter, usually found near the bottom of snow pack)

Hardness (use gloves)
Soft (4 fingers)*
Medium hard (1 finger)*
Hard (pencil)*
Very hard (knife)*

*The object indicated (but not the foregoing one) can be pushed into the snow without considerable effort.

Wetness (use gloves)
Dry (snowball cannot be made)
Moist (does not obviously contain liquid water, but snowball can be made)
Wet (obviously contains liquid water)
Slushy (water can be pressed out)

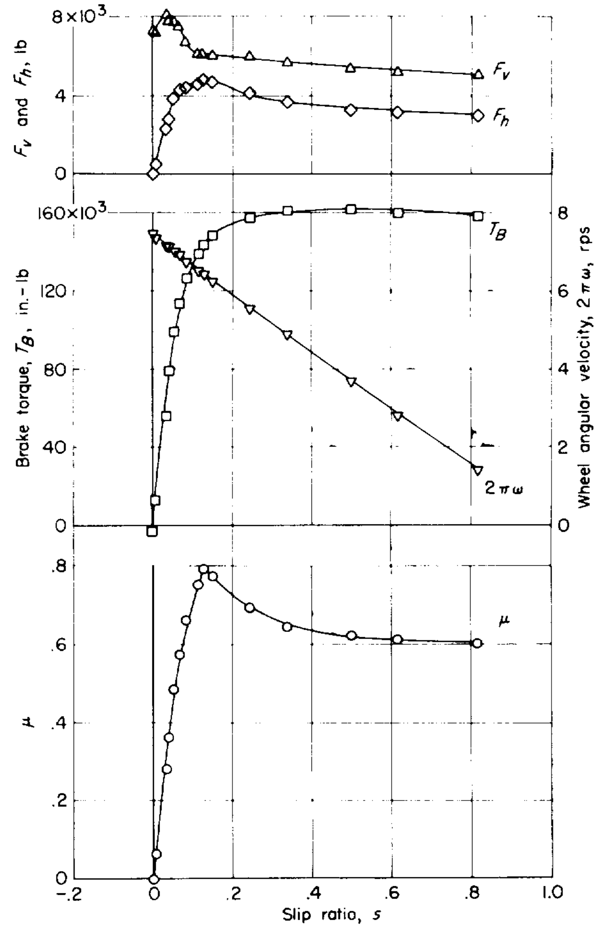

FIGURE 6. Typical variation of vertical and horizontal ground-reaction forces, brake torque, wheel angular velocity, and coefficient of friction with slip ratio measured in braking of the C-123B airplane on a dry surface.

RESULTS AND DISCUSSION

Typical curves for the variation of the vertical and horizontal ground-reaction forces, the brake torque, the wheel angular velocity, and the coefficient of friction with the slip ratio during one braking cycle are shown in figure 6. Results are shown only for the portion of the cycle during which the brake torque was increasing (with resulting decrease in the wheel speed). Results for the remainder of the cycle, during which the brake torque was released and the wheel spun up, were found to be unreliable because the rapidity with which this part of the cycle occurred was too high for the frequency-response characteristics of the instrumentation. It can be seen in figure 6 that as the brake torque is applied, the coefficient of friction increases to a maximum at a slip ratio of 0.125; with further increase in brake torque, the coefficient of friction decreases. Most investigators believe that the slip of the wheel for the part of the curve prior to the peak is primarily the result of the stretching of the rubber in the footprint of the tire. Beyond the peak, adhesion between the tire and surface deteriorates with progressing amounts of skidding until, at a slip ratio of 1.0, full sliding occurs that is, the wheel is locked.

It can be realized from the results given in figure 6 that the minimum stopping distance would be attained by using the correct amount of brake torque to give the peak value of friction coefficient at all times during the braked landing roll.

Operation of the braked wheel at slip ratios greater than that for maximum friction coefficient (incipient-skidding condition) not only increases the stopping distance but, because of the skidding, increases tire wear. In an attempt to make use of the maximum value of friction coefficient, various antiskid devices have been developed and are in current usage. For these reasons, most of the results presented in this paper are concerned with the maximum value of the coefficient of friction.

MAXIMUM FRICTION COEFFICIENT

Dry surfaces. The variation of the maximum values of friction coefficient μ_{max} with ground speed for a dry portland-cement concrete runway and for three dry bituminous pavements is given in figures 7(a) and 7(b). For both types of dry pavements, it can be seen that the mean value of μ_{max} is about 0.8, and no marked variation with speed is evident over the ranges tested. Results could not be obtained at speeds lower than those

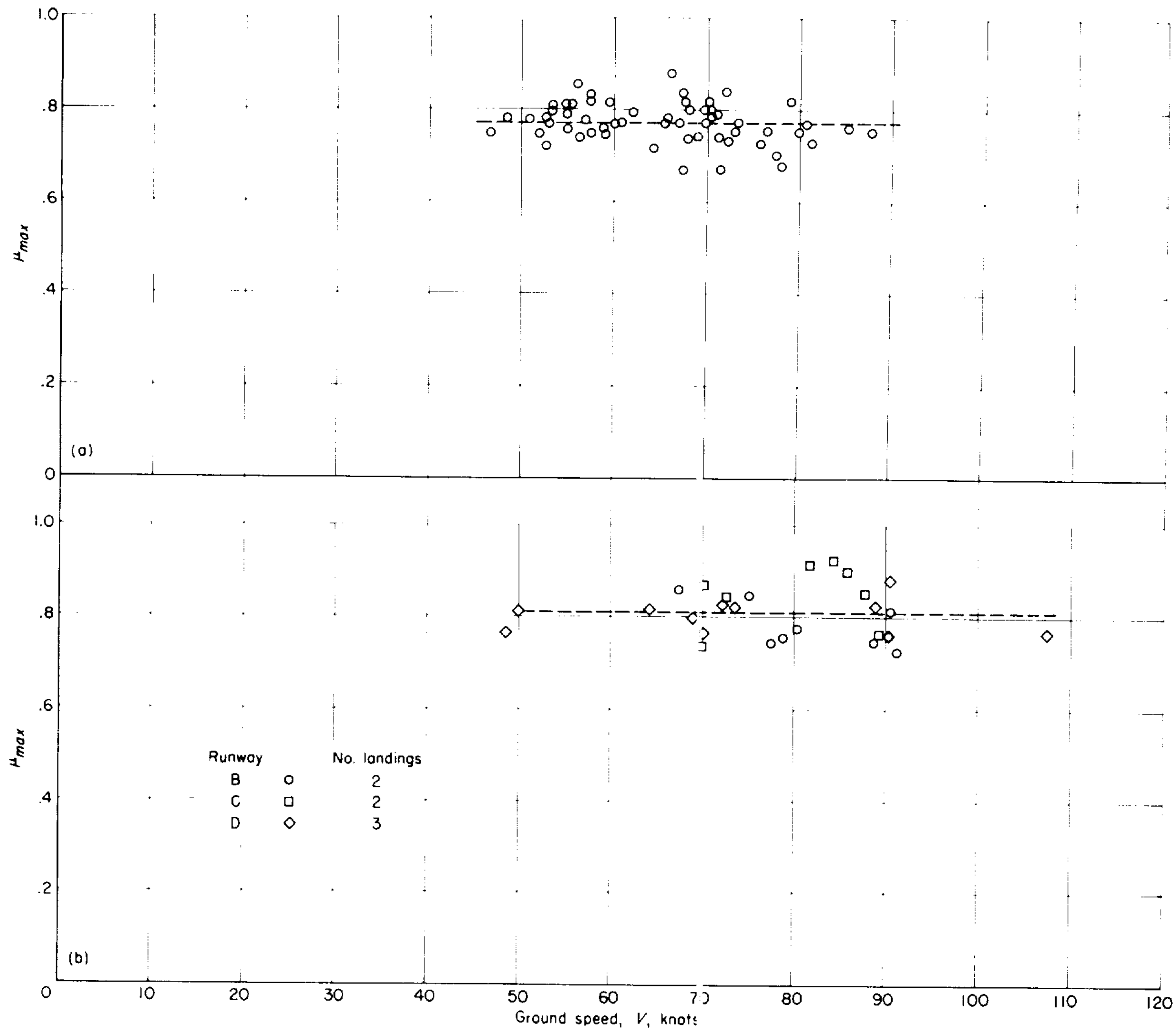

(a) Runway A; dry portland-cement concrete; five landings.

(b) Runways B, C, and D; dry bituminous pavements.

FIGURE 7. Variation with ground speed of maximum values of tire-friction coefficient measured in braking of the C-123B airplane on various dry runways. The vertical force F_v ranged from 1,900 to 9,600 pounds.

shown because the maximum brake-torque capability was insufficient to develop the maximum horizontal force available at the increased vertical loads. The spread in values of μ_{max} for the dry surfaces is believed to be caused by the effects of such parameters as tire temperature, surface roughness, and surface deposits such as skid marks. Over the range of F_v covered in the tests (1.9×10^3 to 9.6×10^3 pounds), no effect of vertical load could be determined from examination of the results for the concrete surface. Comparison of the results for the dry bituminous pavements with the surface-roughness pictures (fig. 5) does not reveal any significant effects of roughness on the friction coefficient.

Snow-covered surfaces.—The variation of μ_{max} with ground speed on seven different snow-covered runways is given in figure 8. Considerable variation in the mean values of μ_{max} for the different runways is evident, the mean values ranging from 0.25 up to 0.37. It appears that, in general, the lower mean values are associated with an icy subsurface, while the higher mean values occur when the subsurface is for the most part bare pavement. These results appear to indicate that the tire is breaking through the upper snow deposit during braking and the subsurface thus has considerable effect on the value of μ_{max}.

A special case illustrating the effect of breakthrough on μ_{max} occurred with runway I (fig. 8(e)) where higher values of μ_{max} are clearly evident during several cycles for the left gear. These higher values are believed to be the result of the occasional breakthrough to the bare pavement which was noted on examination of the airplane tracks. Photographs of the tracks made with the roughness camera for breakthrough to the icy packed-snow subsurface and to the bare pavement are shown in figures 5(h) and 5(i). For this test the right gear, which was operating in the deeper snow at the edge of the runway, had less tendency to break through than the left gear.

The influence of the subsurface on μ_{max} is evident also for runways F and G (figs. 8(b) and 8(c)). On runway F it was noted that the airplane tires generally cut through to the bituminous surface, which apparently resulted in the relatively high mean value of μ_{max}. The two low points at speeds of about 59 and 62 knots are probably the result of breakthrough to an icy patch. On runway G it was noted that the airplane tires occasionally cut through to either bituminous or ice subsurface, which explains the greater variation of μ_{max} for this test than for the other tests on snow-covered surfaces.

For the ranges covered in the tests, speed appeared to have little or no effect on the value of μ_{max}. Variations in snow depth, age, hardness, moistness, and treatment had no distinguishable effect on μ_{max}. Similarly, no effect of surface temperature on μ_{max} is evident for the range of surface temperature covered in the tests (3° F to 32° F). (See table I.)

Ice surface.—The variation of μ_{max} with ground speed for test on the ice runway prepared on the frozen lake surface is given in figure 9 for two surface temperatures. It can be seen that the mean value of μ_{max} for both the subfreezing surface temperature (19° F) and the freezing-point surface temperature is about 0.18, and no dependence on speed is evident over the speed range covered. It is believed that the value of μ_{max} in these cases is probably limited primarily by the shearing strength of the ice. For the case with the surface temperature at the melting point, it should be pointed out that no film of water was observable on the runway surface. The lack of an appreciable film of water may well be the reason for the agreement of μ_{max} values at the two surface temperatures; for two ice surfaces which differ in that one is covered by an appreciable film of water, the μ_{max} values may differ markedly.

Wet surfaces.—The variation with ground speed of μ_{max} for six different wet surface conditions is given in figure 10. Parts (a), (b), and (c) of this figure show results for wet portland-cement concrete and parts (d) and (e) show results for wet bituminous pavement. The approximate mean value for the dry pavement, taken from figure 7, is shown in each part of figure 10 for comparison. Since the conditions for these wet-surface tests were continually changing, it was not possible to make repeat landings, and hence the number of cycles obtained for each condition is limited. Also, since surface conditions were found to be different for each main wheel, the results for the two wheels are presented separately.

It can be seen in figure 10 that the values of μ_{max} were, in general, considerably lower for the wet surfaces than for comparable dry surfaces.

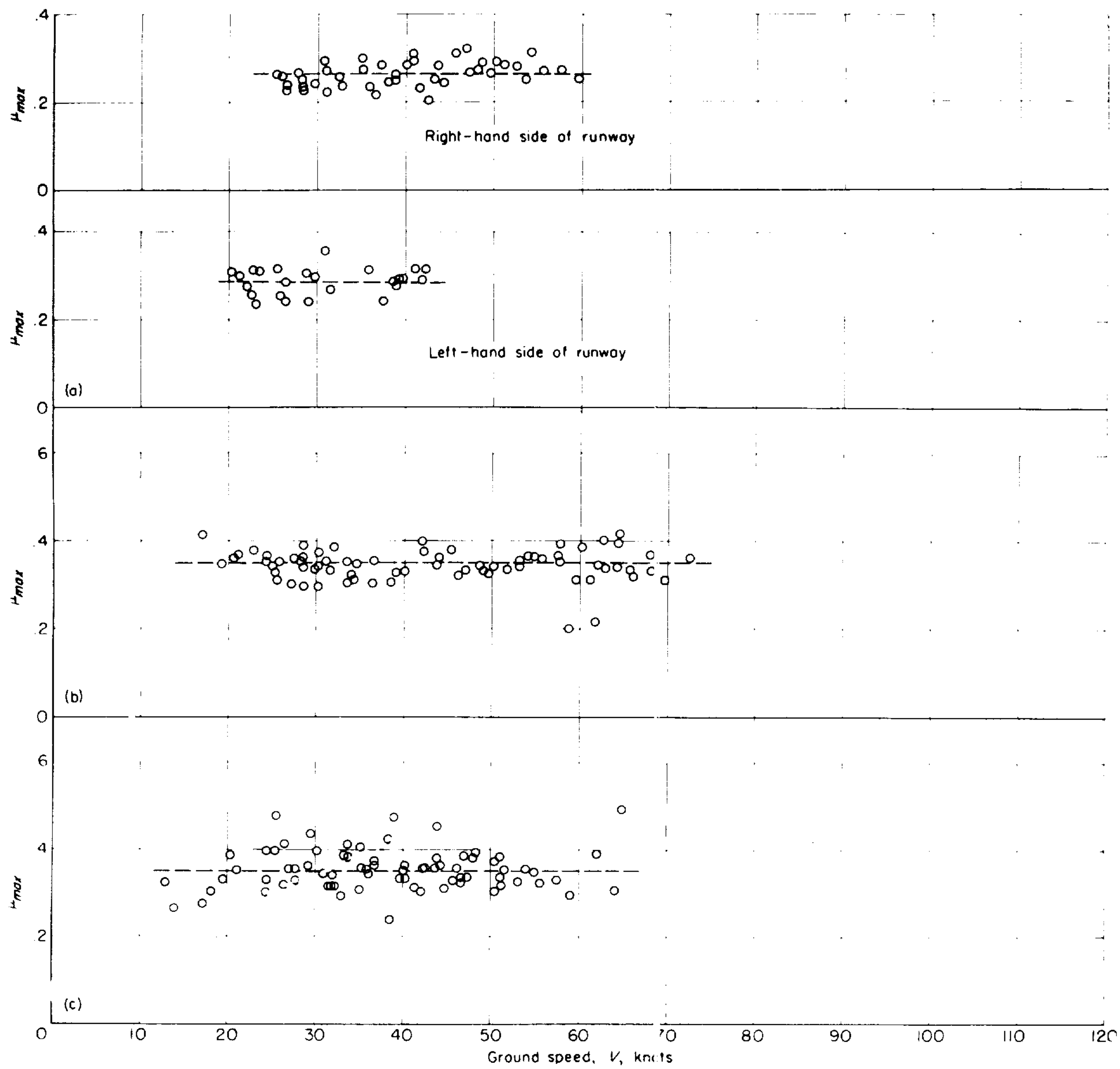

(a) Runway E; 1/4 to 1/2 inch new, soft, moist snow over icy, refrozen snow subsurface; two landings.

(b) Runway F; 1/4 to 1/2 inch new, moist snow, hard-packed by recent plowing, over bituminous pavement; two landings.

(c) Runway G; 5 to 6 inches new, soft, dry snow with 1/16-inch crust over ice-spotted bituminous pavement; two landings.

FIGURE 8. Variation with ground speed of maximum values of tire-friction coefficient measured in braking of the C-123B airplane on various snow-covered runways. The vertical force F_v ranged from 4,100 to 22,000 pounds.

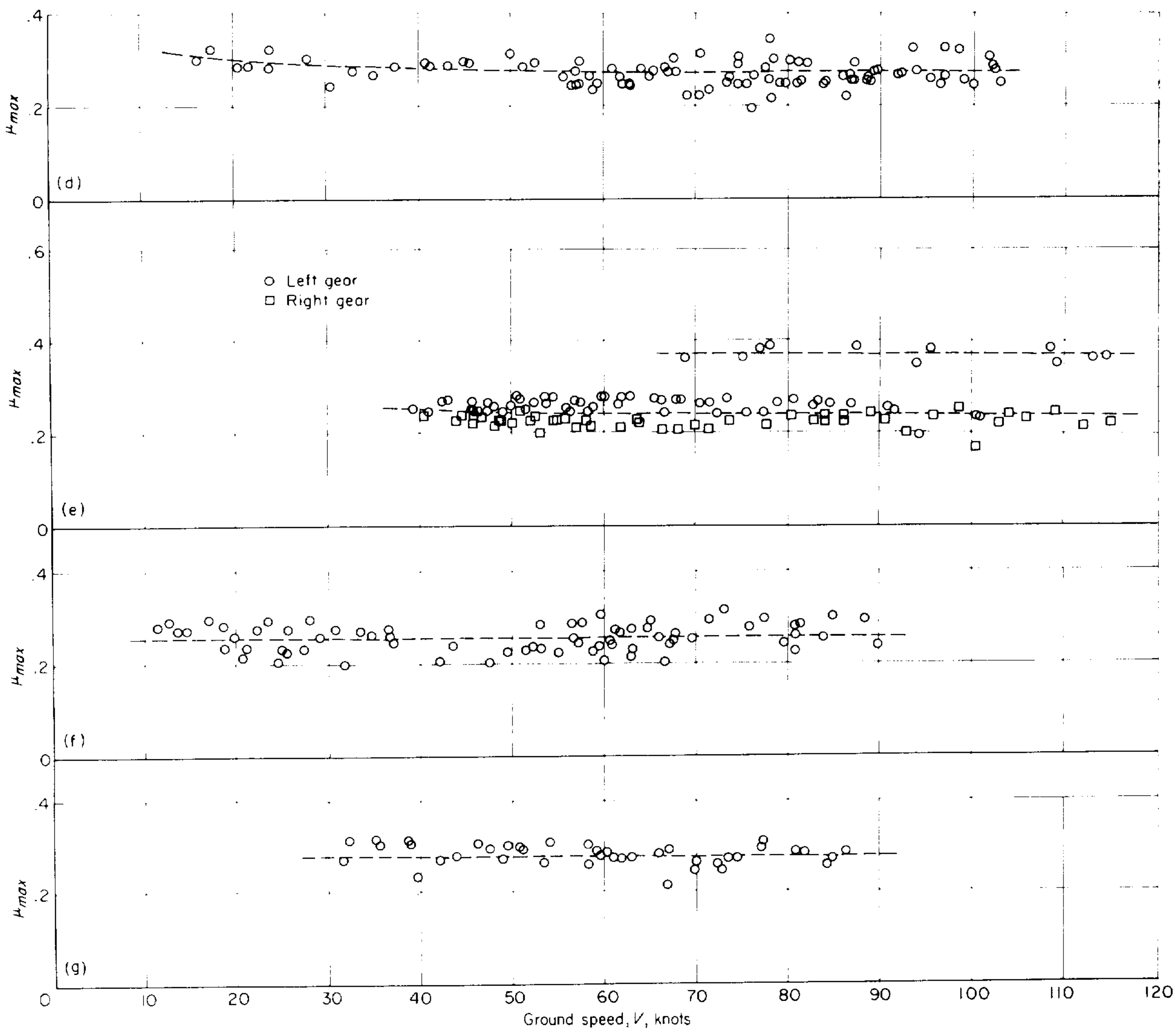

(d) Runway H; 1 to 2 inches new, soft, dry snow over icy, packed snow subsurface; three landings.

(e) Runway I; 1 to 4 inches new, soft, moist snow over icy, packed snow subsurface; two landings.

(f) Runway J; 5 inches old, soft-to-hard, moist-to-wet snow left on frozen lake surface when top 7-inch layer removed by ploughing; three landings.

(g) Runway K; 1 to 3 inches new, soft, dry snow over 5 inches old, hard, dry snow left on frozen lake surface by previous ploughing operation; one landing.

FIGURE 8. Concluded.

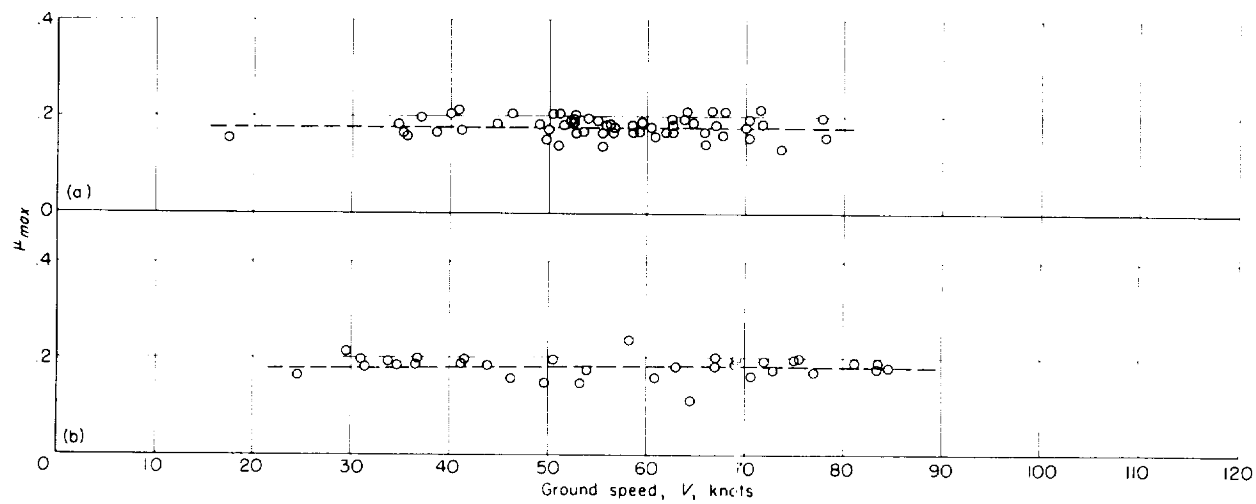

(a) Surface temperature 32° F; three landings.
(b) Surface temperature 19° F; one landing.

FIGURE 9. Variation with ground speed of maximum values of tire-friction coefficient measured in braking of the C-123B airplane on runway L. Frozen lake surface; thin, patchy snow residue left on ice from ploughing operation. The vertical force F_v ranged from 5,500 to 23,100 pounds.

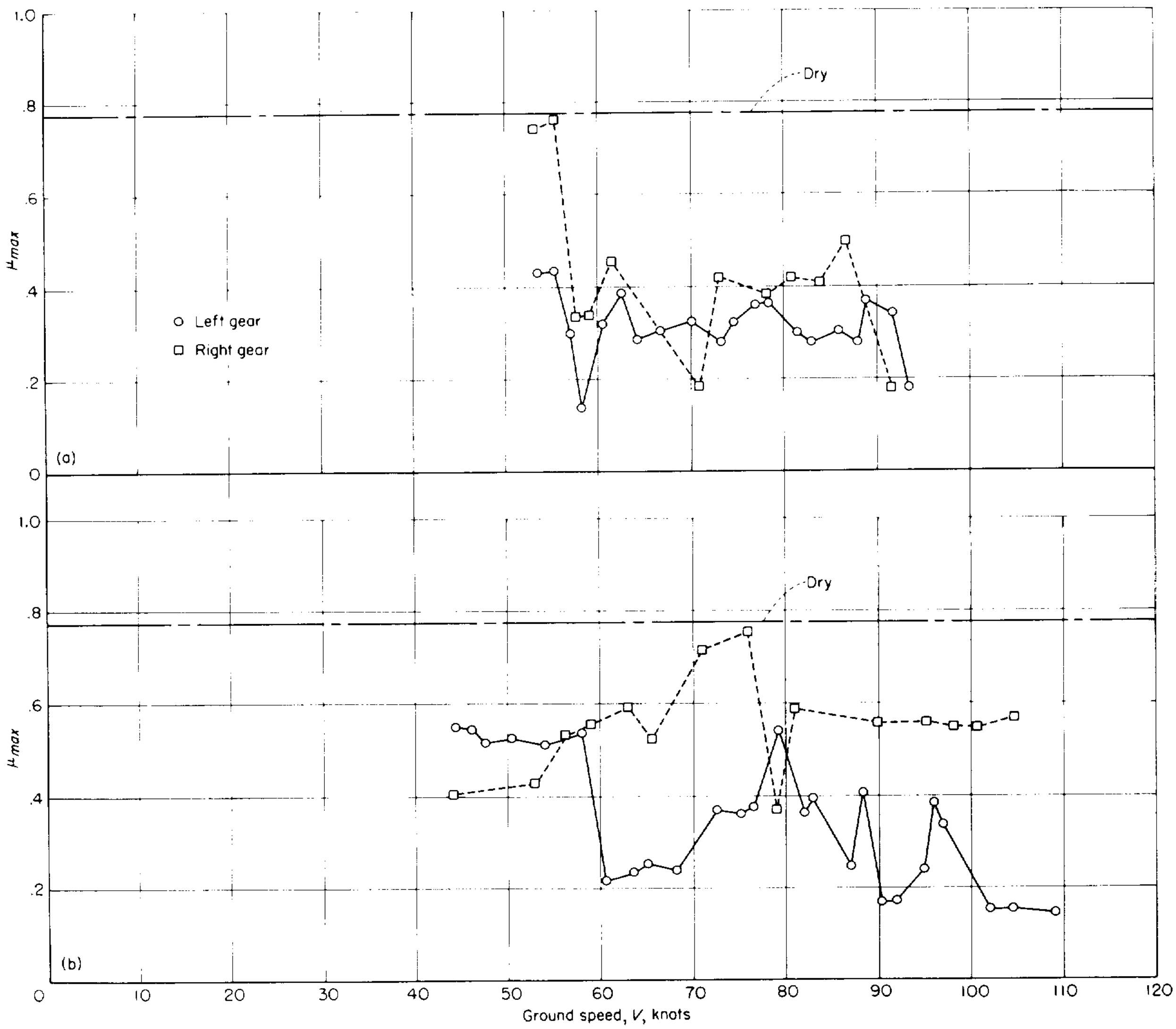

(a) Runway A (east end); wet portland-cement concrete; landing made during light rain (0.02 inch per hour) just after 0.16 inch of rain had fallen in previous 40 minutes.

(b) Runway A (west end); wet portland-cement concrete; landing made during light rain (0.02 inch per hour) about 15 minutes after end of 0.16-inch rainfall in a 40-minute period.

FIGURE 10.—Variation with ground speed of maximum values of tire-friction coefficient measured in braking of the C-123B airplane on various wet runways. The vertical force F_v ranged from 1,500 to 13,100 pounds.

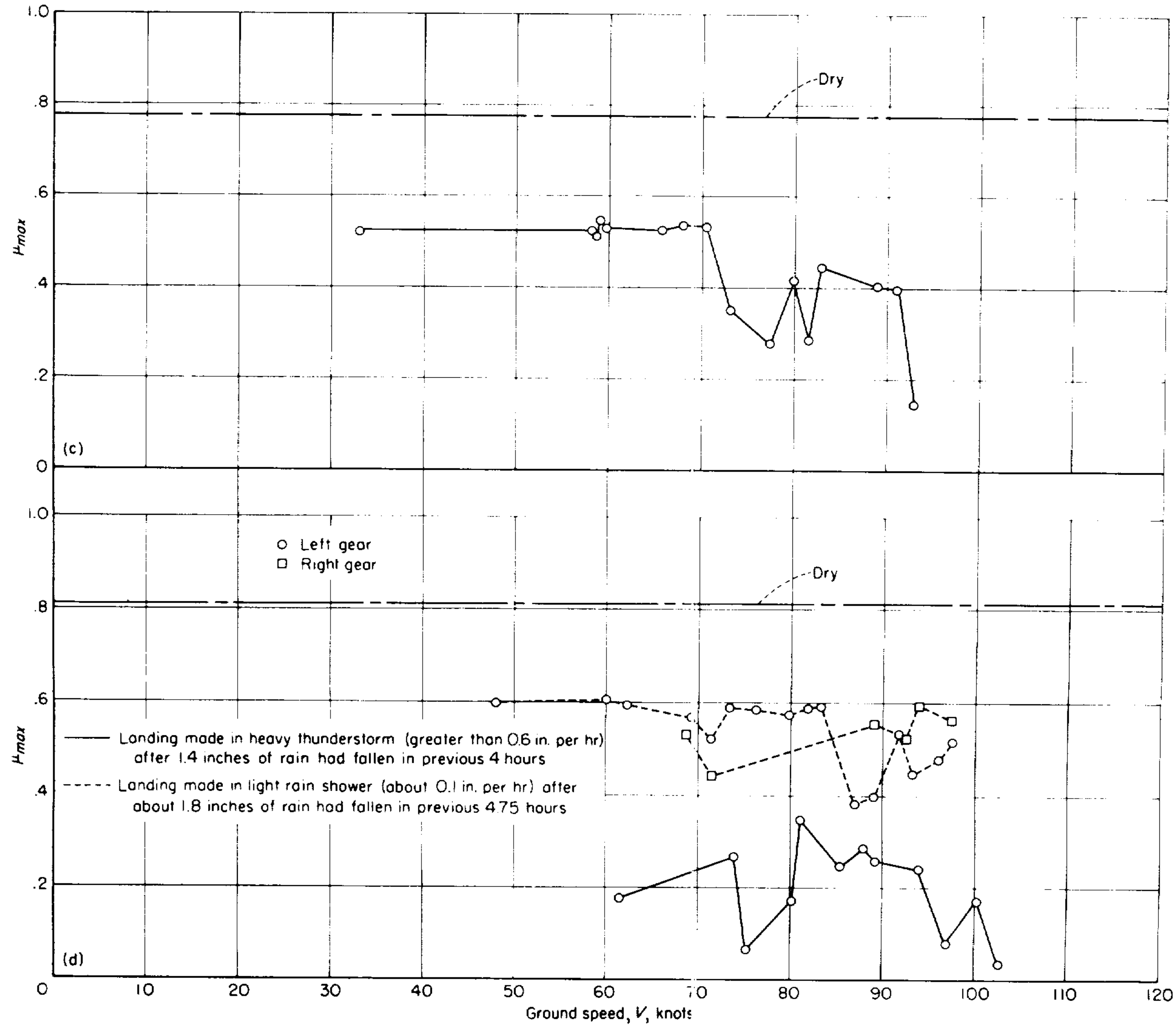

(c) Runway M; wet portland-cement concrete; landing made just after end of a 2-hour period of light-drizzle to light-rain conditions.

(d) Runway D; wet bituminous pavement.

FIGURE 10.—Continued.

The values of μ_{max} for the wet surfaces, however, varied from as low as 0.04 to over 0.80. These variations are ascribed primarily to various depths of water along the runway, the lower values of μ_{max} being associated with the greater depths of water. The effect of water depth can be seen by comparing the μ_{max} values obtained in the landing made in a heavy thunderstorm, when considerable water was evident on the runway, with those obtained in the landing made three-fourths of an hour later during a light rain shower, when less water was present (fig. 10(d)). The effect of the depth of water on μ_{max} is further evident from the results in figure 10(e) which indicate that, for a runway which had water deep enough to cover the surface projections only in occasional shallow puddles, the values of μ_{max} obtained were about the same as those for a dry surface except for the occasional lower value obtained when the wheel apparently passed through a puddle.

The relatively low values of μ_{max} found on wet surfaces are believed to be associated with partial-to-full loss of contact between the tire and the surface in the footprint area by interposition of a layer of water. With full loss of contact in the

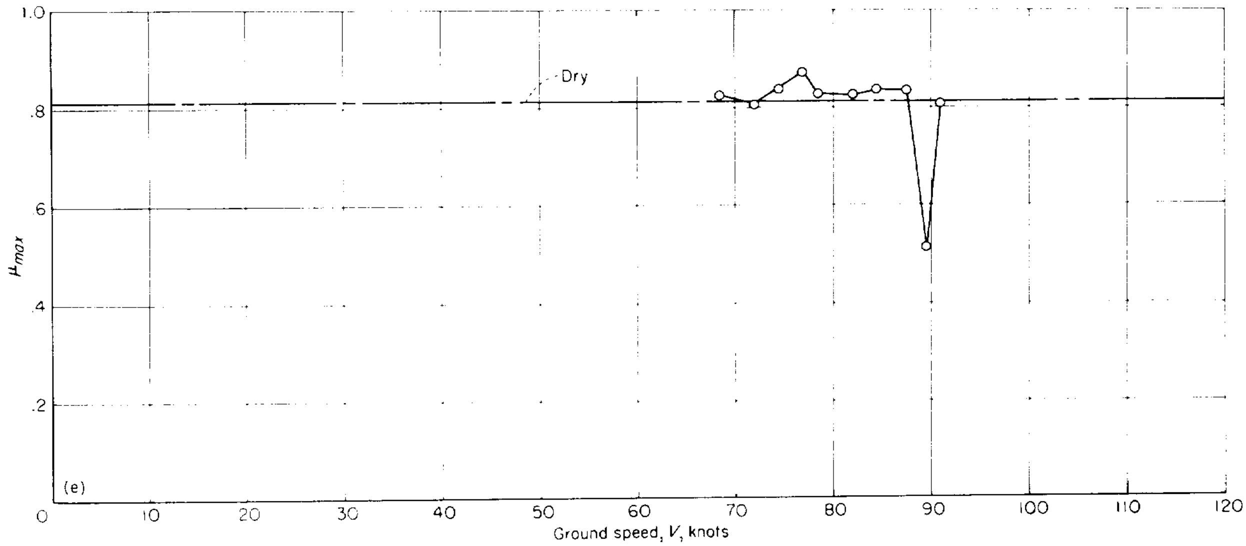

(e) Runway N: wet bituminous pavement; landing made in light drizzle with runway still wet from previous rain and dotted with shallow puddles.

FIGURE 10.—Concluded.

footprint area the tire is, in effect, planing on the surface of the water. (This process could possibly also be analogous to perfect lubrication in a bearing.) It appears that, under wet conditions, in order for the tire to make contact with the solid runway surface it must first force the water out of the way. That is, the tire exerts pressure on the water in the footprint area and ejects it, generally out to the side. However, because of the inertia of the water and viscous effects, this process takes time. As the forward speed of the tire is increased the tire travels farther in the time required to eject the water, and therefore the water penetrates farther along the footprint or contact area of the tire. The area of the footprint in contact with the solid surface is thereby reduced, and consequently the friction coefficient that can be developed is decreased. Ultimately, if the speed becomes high enough, the water will penetrate the full length of the footprint and all contact with the solid runway surface will be lost, leaving only the relatively insignificant retarding forces that can be exerted by the water. An elementary analysis of this process, without consideration of viscous effects, indicates that for a given water depth and surface texture the distance of penetration of the water under the footprint of the tire is proportional to the forward speed and the width of the tire footprint and inversely proportional to the square root of the tire pressure. That is, the coefficient of friction that can be developed on a given wet surface would be expected to decrease with increase in forward speed, with increase in ratio of footprint width to length, or with decrease in tire pressure.

An interesting effect of the extremely low friction coefficients that can be encountered with wet surfaces is illustrated in figure 11, which gives time histories of the slip ratio, brake torque, and friction coefficient during a braked landing on a wet portland-cement concrete runway. It is seen that, after the brake torque is released by the antiskid device, the wheel tends to remain in a partially skidding condition for a considerable time before spinning up or until the wheel slip is reduced sufficiently to allow another braking cycle to occur. During the partial skidding a very low friction coefficient (in general, less than 0.1) exists. The resultant moment on the wheel from the combined action of the frictional force and the pressure forces of the water is apparently small under these conditions and the spin-up is slow. Similar effects have been demonstrated with a model wheel subjected to the action of water forces on a treadmill apparatus (ref. 10).

FULL-SKID FRICTION COEFFICIENT

Through inadvertent locking of one wheel by temporary malfunction of the antiskid device, some full-skid friction coefficients were obtained

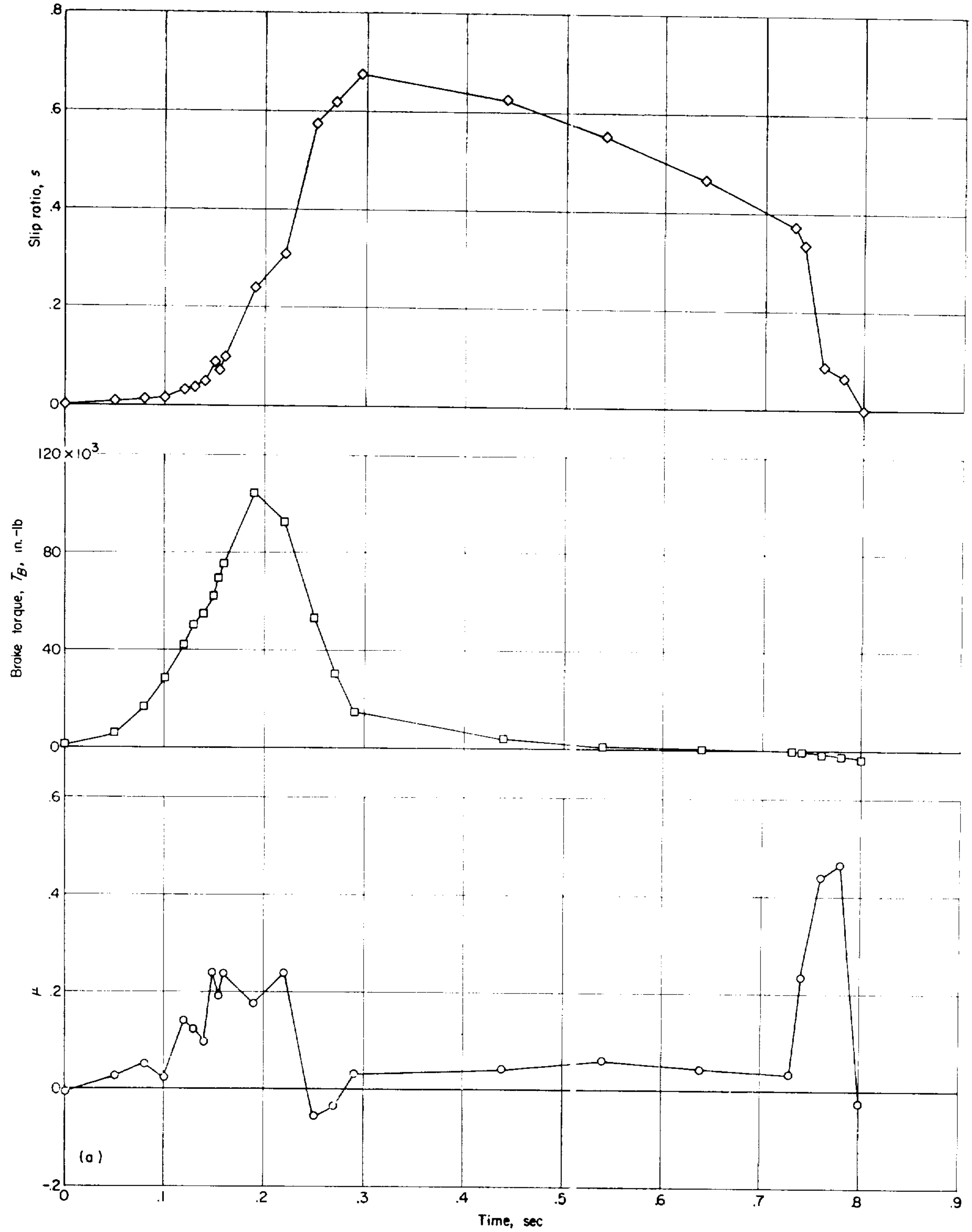

(a) Average ground speed $\overline{V}$ = 91 knots.

FIGURE 11.—Variation of tire-friction coefficient, brake torque, and slip ratio with time for one wheel of C-123B airplane during partial skidding on wet portland-cement concrete runway.

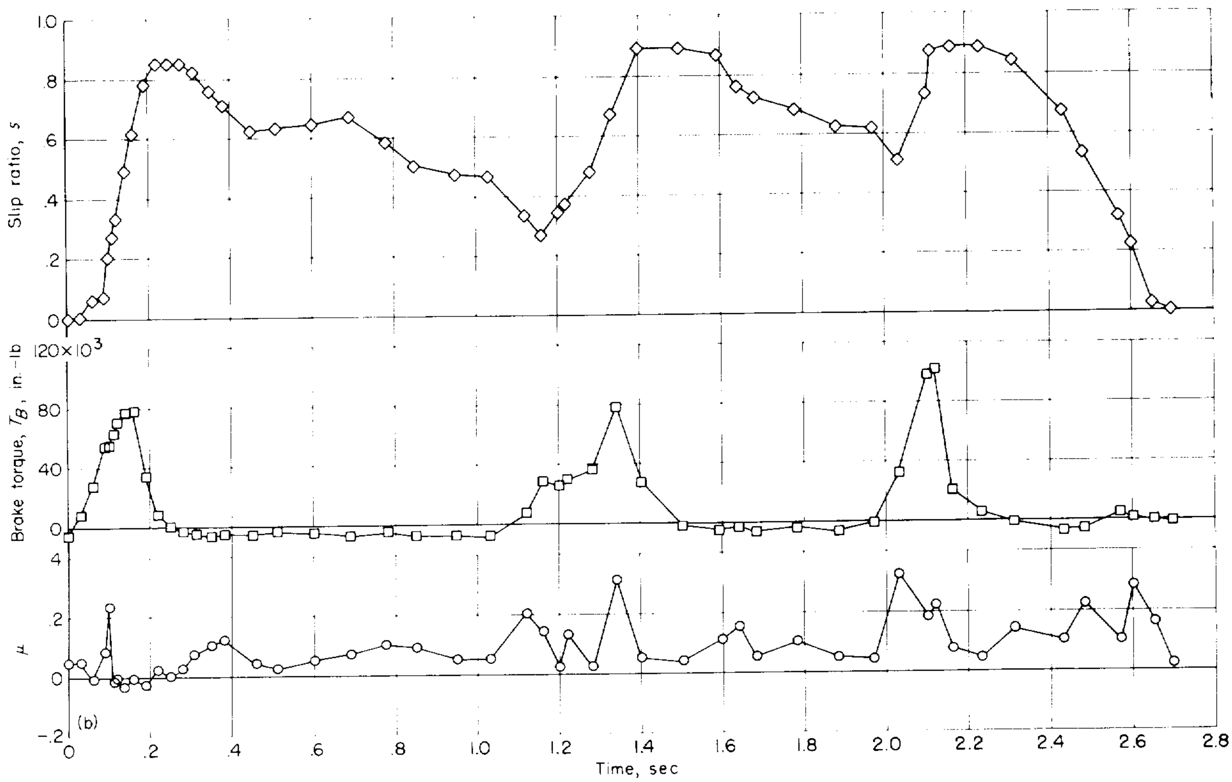

(b) Average ground speed $\overline{V}$ = 67 knots.

FIGURE 11.—Concluded.

on a dry portland-cement concrete runway, a snow-covered runway, the frozen lake surface, and two wet surfaces. These results are shown in figure 12. Except on the wet surfaces, the full-skid friction coefficient decreased in general as the skid continued, reaching values between about 0.1 and 0.2. This decrease is believed to have been caused primarily by heating associated with the frictional forces. For the dry surface, the result was a "burning" skid ending with a blowout.

For the skidding wheel on the wet surfaces (fig. 12(d)) the full-skid friction coefficient was apparently near zero at the beginning of the skid—that is, at the higher speeds. As the speed decreased, the full-skid friction coefficient increased to a value of about 0.3 at the lower speeds. The extremely low values of the full-skid friction coefficient, especially at the higher speeds, are believed to be associated with planing of the tire on the water, as has been previously discussed. It appears that the effect of the water on the full-skid friction coefficient decreases as the speed decreases. This decrease in the effect of the water is also in agreement with the model tests referred to previously (ref. 10).

RELATION OF FRICTION TO WHEEL SLIP

The relation between the tire-to-surface friction and the wheel slip ratio in braking is important to the understanding of the stress and strain developed in the tire contact area (ref. 11) and is also important in the development and design of antiskid devices. Examples of the relationship between the coefficient of friction and the slip ratio for some of the surfaces tested are given in figure 13. For the dry portland-cement concrete (fig. 13(a)) the coefficient of friction increases fairly linearly with slip ratio up to a well-defined peak, and beyond the peak it decreases rather slowly with further increase in slip ratio. It is not known whether the differences in the variation of the coefficient of friction with slip ratio below the peak values of μ are caused by such factors as vertical load, tire temperature, and speed or occur as a result of the limits of accuracy in the measurement of slip ratio. It should be noted, however, that the peak values of μ all occur within a narrow band of slip ratio.

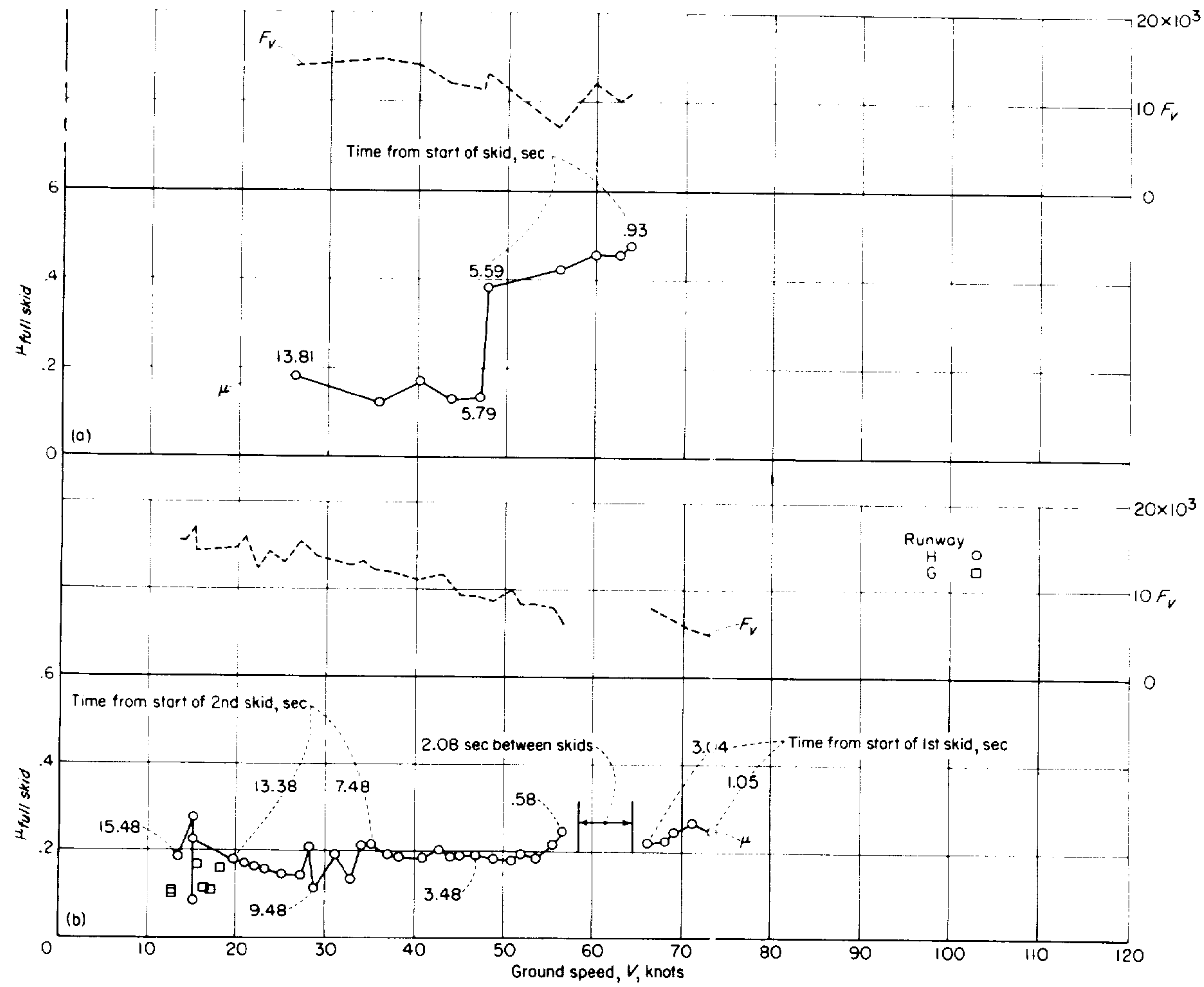

(a) Dry portland-cement concrete (runway A).
(b) Snow-covered runways.

FIGURE 12. Variation with ground speed of full-skid tire-friction-coefficient values measured in braking of the C-123B airplane on runways having various surface conditions. Vertical-load variation is also shown.

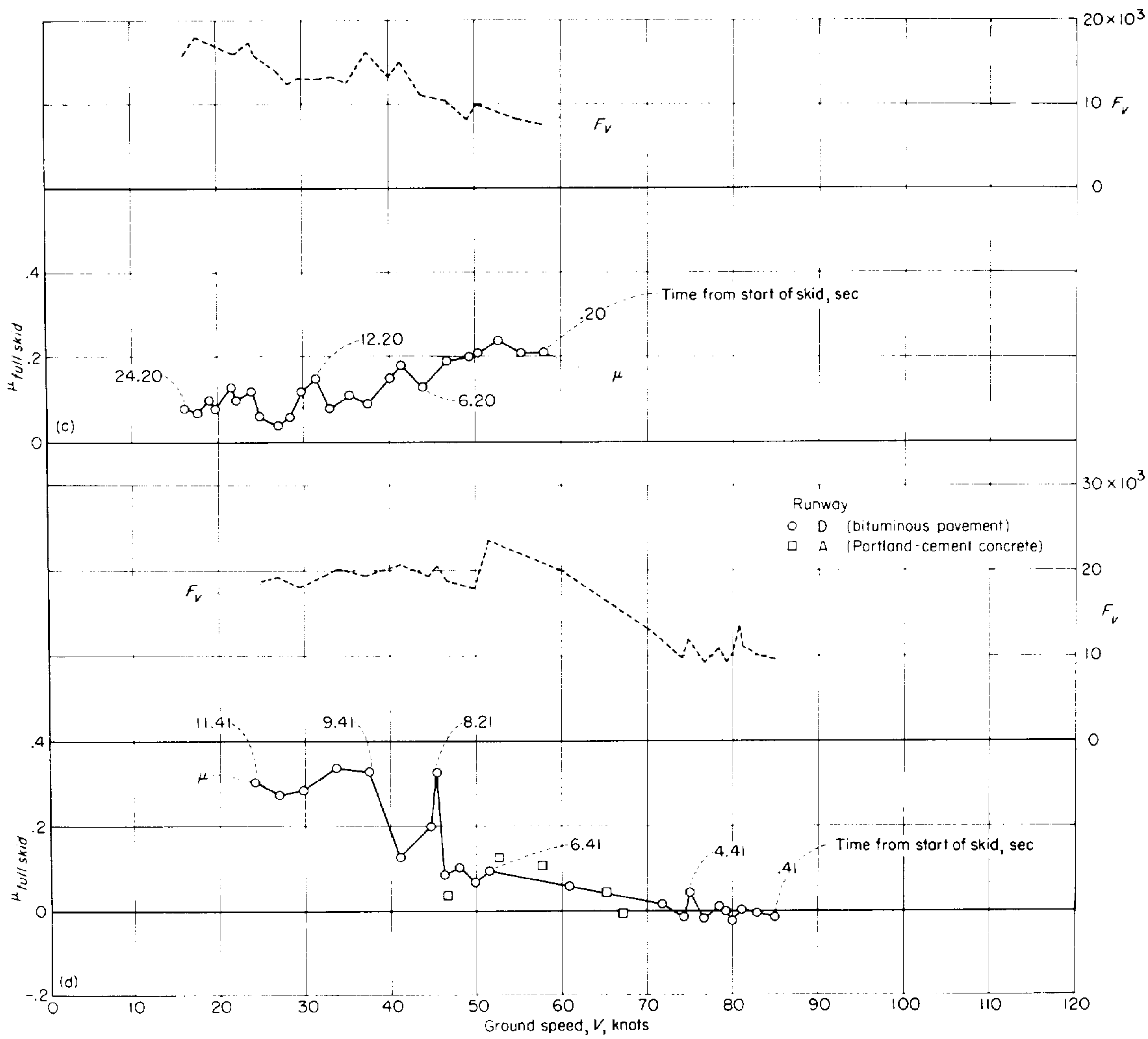

(c) Frozen lake surface (runway L).
(d) Wet surfaces.

FIGURE 12. Concluded.

In contrast to the dry-surface results, the friction-slip relationship for the surface covered with deep snow (fig. 13(b)) has a less linear initial slope and, in general, a more rounded peak, with the slip ratio for the peak value varying over a large range. With less snow (for example, fig. 13(c)), a more linear slope of the increasing part of the curve is apparent, but both well-defined and rounded peaks are evident. The friction-slip relationship for the results on the ice surface (fig. 13(d)) appears to be characterized by a rather linear increase up to a sharp peak, and a rapid decrease in value beyond the peak. In some cases, extremely low values of μ apparently occur at rather low values of slip. For the wet surfaces (figs. 13(e) and 13(f)), the increasing part of the curve appears to be fairly linear, as was the case for the dry surface, and the peaks also appear to be well defined. The decrease in μ beyond the peak, however, is much more rapid than for the dry surface.

SLIP RATIO FOR MAXIMUM FRICTION COEFFICIENT

The slip ratio corresponding to the maximum friction coefficient is of interest in the design of antiskid devices based on holding the wheel at a fixed value of slip ratio during braking. In order to illustrate, for the surfaces tested, the effect of speed on the slip ratio at which the maximum friction coefficient was developed, the slip ratios corresponding to μ_{max} in figures 7 to 10 are presented in figure 14. In the limited speed range covered for the dry surfaces (figs. 14(a) and 14(b)), no effect of speed on the mean value of slip ratio for maximum friction coefficient $s_{max\ \mu}$ was evident. Mean values of 0.1 and 0.075 were obtained for $s_{max\ \mu}$ on the concrete and bituminous surfaces, respectively. For the snow-covered and ice surfaces, however, results were obtained to much lower speeds, and the mean value of $s_{max\ \mu}$ generally increased at the lower speeds. (See figs. 14(c) and 14(d).) For the snow-covered surfaces, mean values of $s_{max\ \mu}$ ranged from 0.03 at high speeds on surfaces with slippery subsurfaces to 0.23 in deep snow on a runway with a bare-pavement subsurface. The $s_{max\ \mu}$ values for the ice surface were similar to those for the snow-covered surfaces with a slippery subsurface. For the wet surfaces (figs. 14(e) and 14(f)), because of the limited amount of data obtained, a rational mean value of $s_{max\ \mu}$ could not be determined.

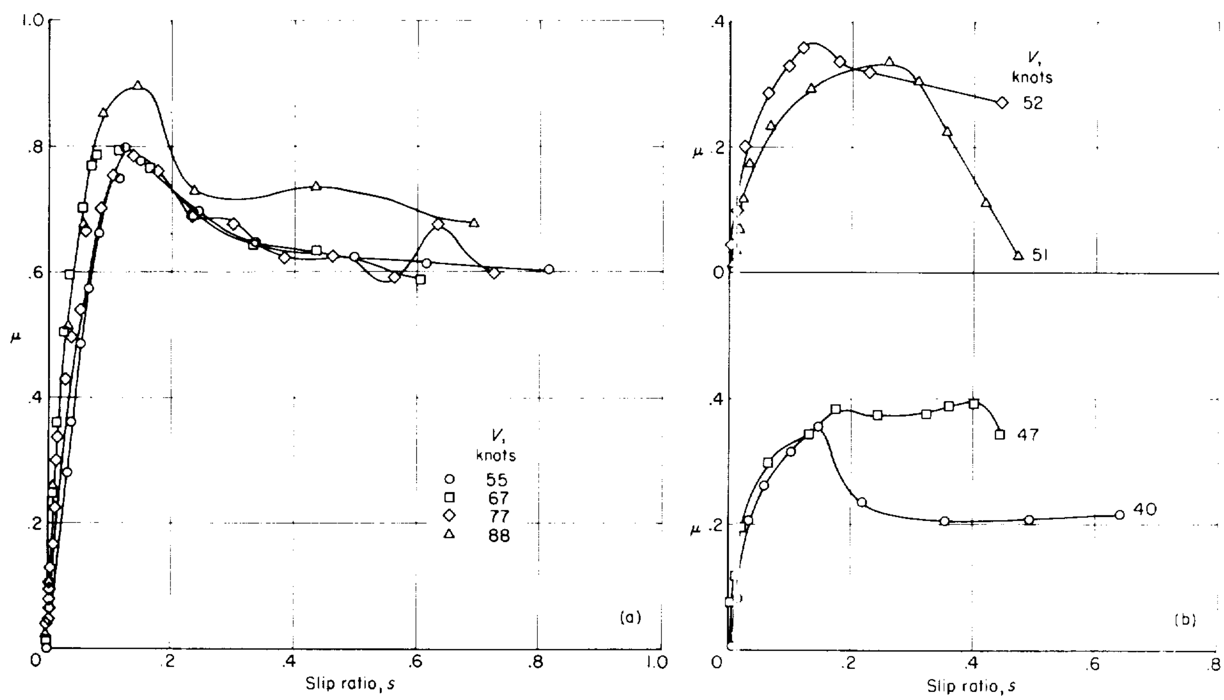

(a) Dry portland-cement concrete (runway A). (b) Five to 6 inches of snow (runway G).

FIGURE 13. Variation of tire-friction coefficient with slip ratio measured in braking with the C-123B airplane on runways having various surface conditions.

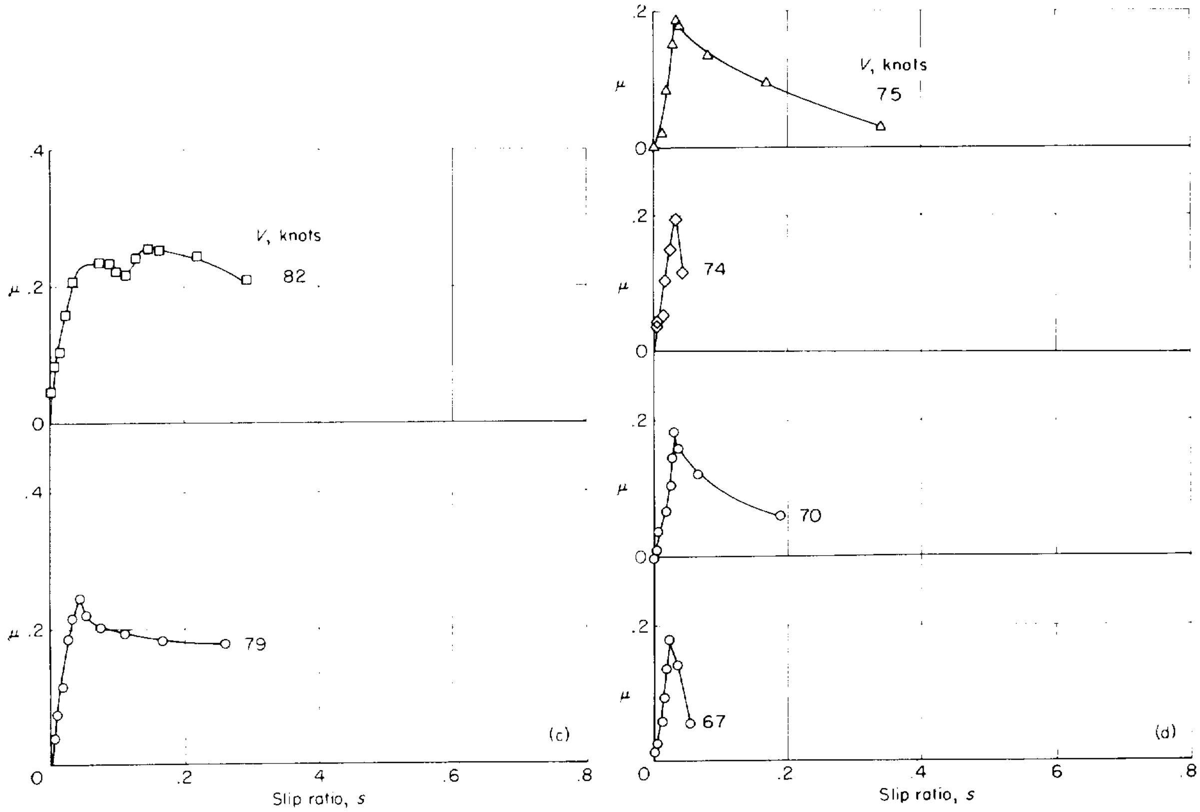

(c) One to 2 inches of snow (runway H).

(d) Frozen lake surface (runway L).

FIGURE 13.—Continued.

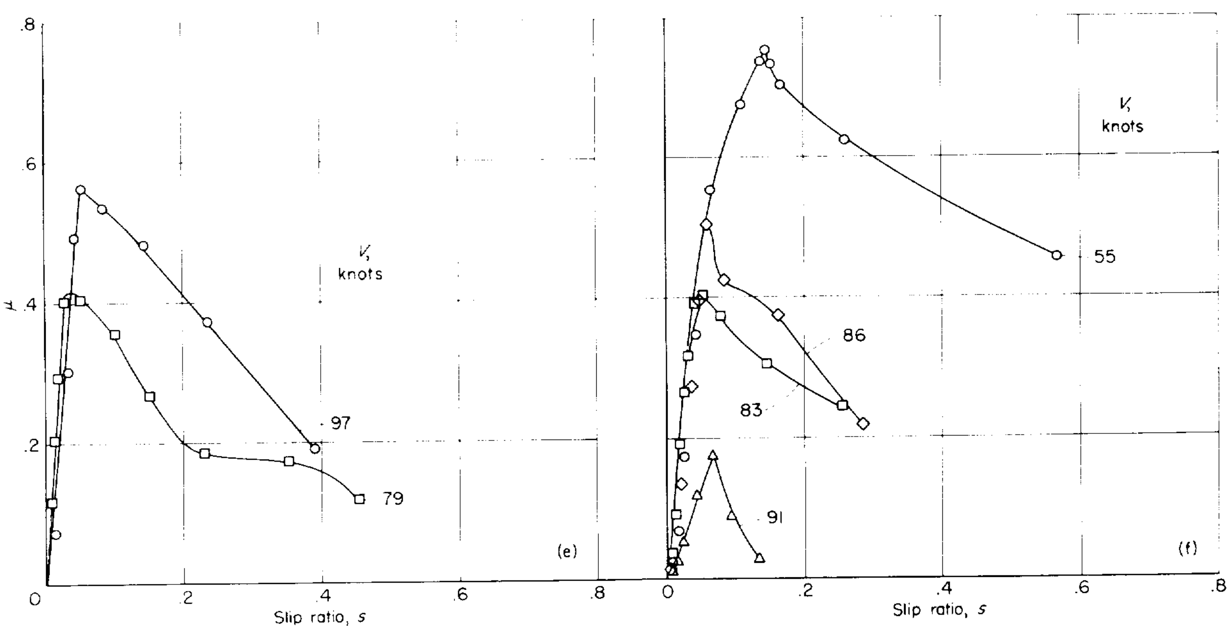

(e) Wet bituminous pavement (runway D).

(f) Wet portland-cement concrete (runway A).

FIGURE 13.—Concluded.

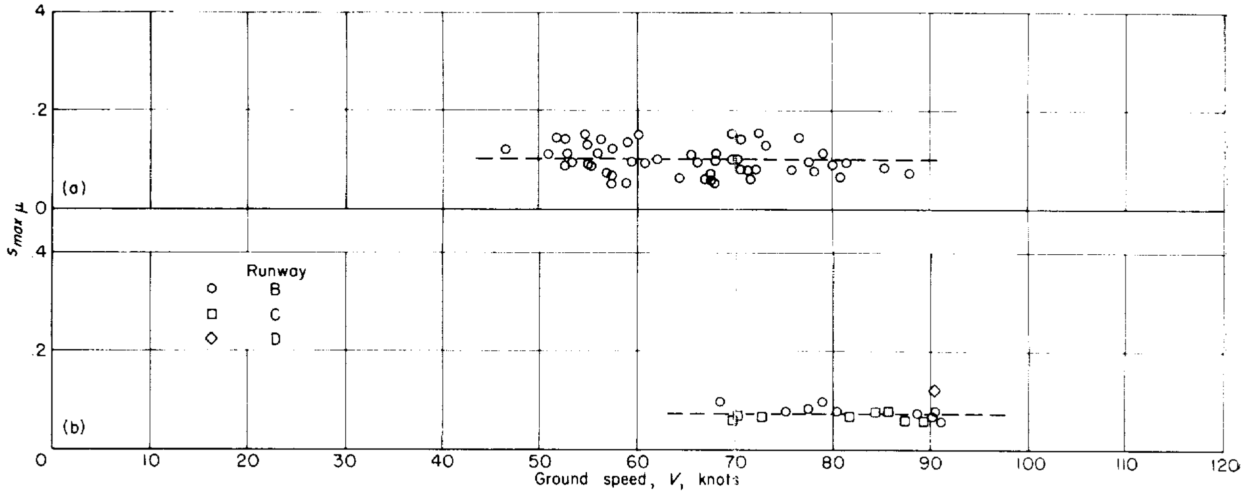

(a) Dry portland-cement concrete (runway A).
(b) Dry bituminous pavements (runways B, C, and D).

FIGURE 14. Variation with ground speed of slip ratio for maximum friction coefficient measured in braking of the C-123B airplane on runways having various surface conditions.

Values of $s_{max\ \mu}$ from 0.02 to 0.26 were obtained on the wet surfaces, this large variation apparently being associated with the large changes in μ_{max} shown previously.

Study of the friction-slip curves (fig. 13) and the slip ratios for maximum friction (fig. 14) indicates that an antiskid device built to operate the wheel at a fixed slip ratio of about 0.10 would generally be successful in developing close to the maximum coefficient of friction available at these speeds for dry and snow-covered surfaces, although in some cases where the peak occurs at a lower slip ratio some excess tire wear might result. For the ice surface, however, a much lower slip ratio (about 0.03 or 0.04) would have to be used at the higher speeds in order to avoid large percentage losses in the friction being developed. For the wet surfaces, the large variation (0.02 to 0.26) in the slip ratio for maximum friction coefficient makes an operational slip ratio difficult to select. It appears from these results, therefore, that a compromise slip ratio (of, perhaps, 0.05) would have to be used for a fixed-slip antiskid device. A device with this slip ratio would result in some loss in stopping distance on all surfaces, compared with a device which could develop the maximum friction force at all times.

CONCLUSIONS

This paper has presented the results of an investigation with the C-123B airplane to determine the tire-to-surface friction coefficients available in braking on both wet and dry concrete and bituminous pavements and on snow-covered and ice surfaces at speeds from 12 knots to 115 knots. Some of the principal results are:

1. The mean value of the maximum friction on both dry portland-cement concrete and dry bituminous pavements was found to be about 0.8, with no effect of speed or load evident over the ranges investigated.

2. For snow-covered surfaces, the mean value of maximum friction coefficient varied from 0.25 to 0.37; the lower values were apparently associated with icy subsurfaces and the higher values with bare pavement subsurfaces. Over the ranges of the investigation, no effects of speed or surface temperature (3° F to 32° F) on the maximum friction coefficient were evident.

3. On an ice surface, the mean value of the maximum friction coefficient was 0.18 at surface temperatures of both 19° F and 32° F, with no apparent dependence on speed.

4. For wet portland-cement concrete and bituminous pavement surfaces, values of maximum friction coefficient varied from 0.04 to more than 0.80. The variations in maximum friction coefficient were believed to be associated primarily with variations in depths of water along the runway. The extremely low values were ascribed to planing of the tire on a film of water.

5. Full-skid (that is, locked wheel) friction co-

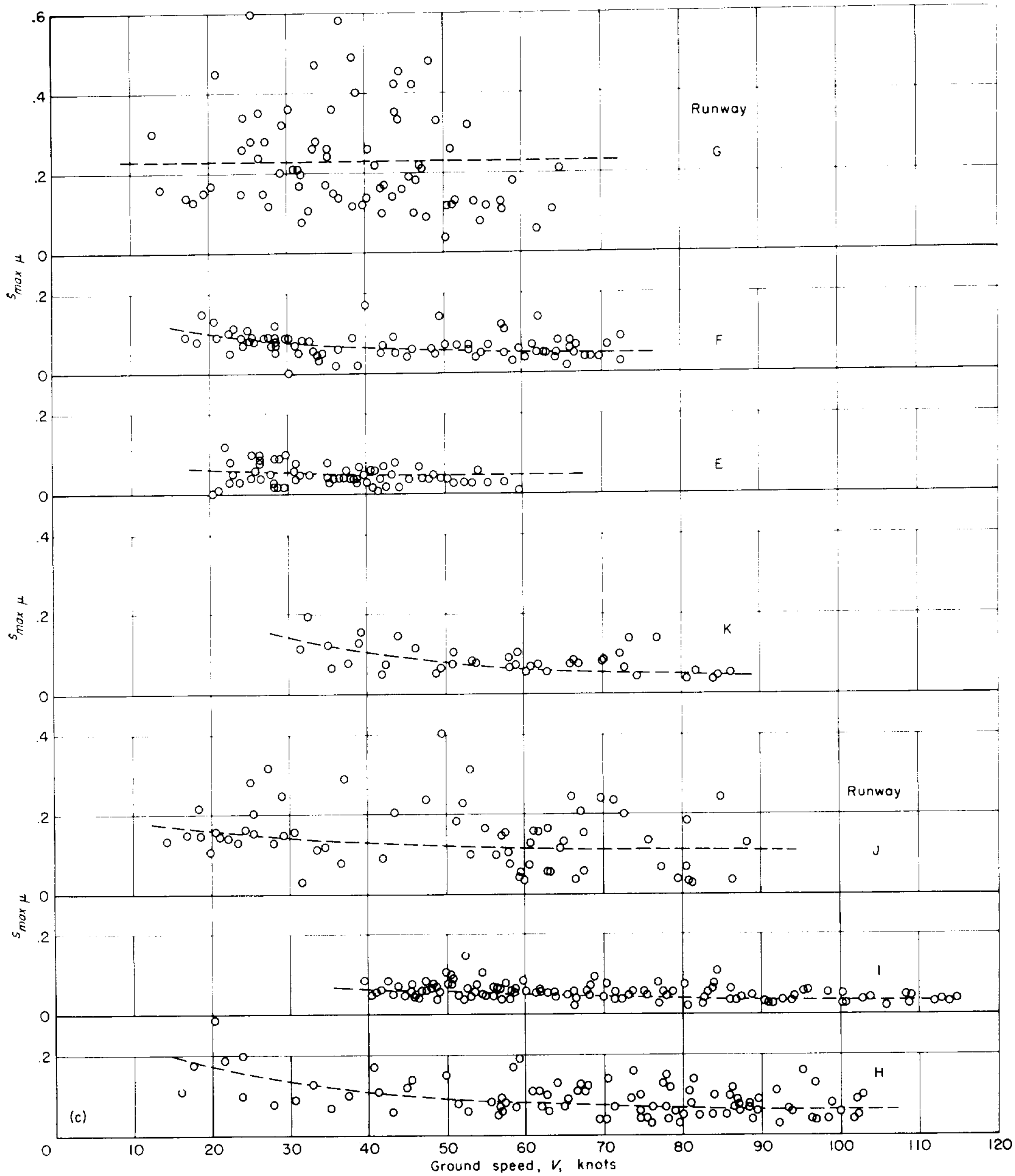

(c) Snow-covered surfaces.

FIGURE 14. Continued.

efficients on the dry, snow-covered, and ice surfaces were found to decrease with decrease in speed as the skid progressed, reaching values between about 0.1 and 0.2. On the wet surfaces, the full-skid friction coefficient was near zero at the higher speeds and increased to about 0.3 as the skid

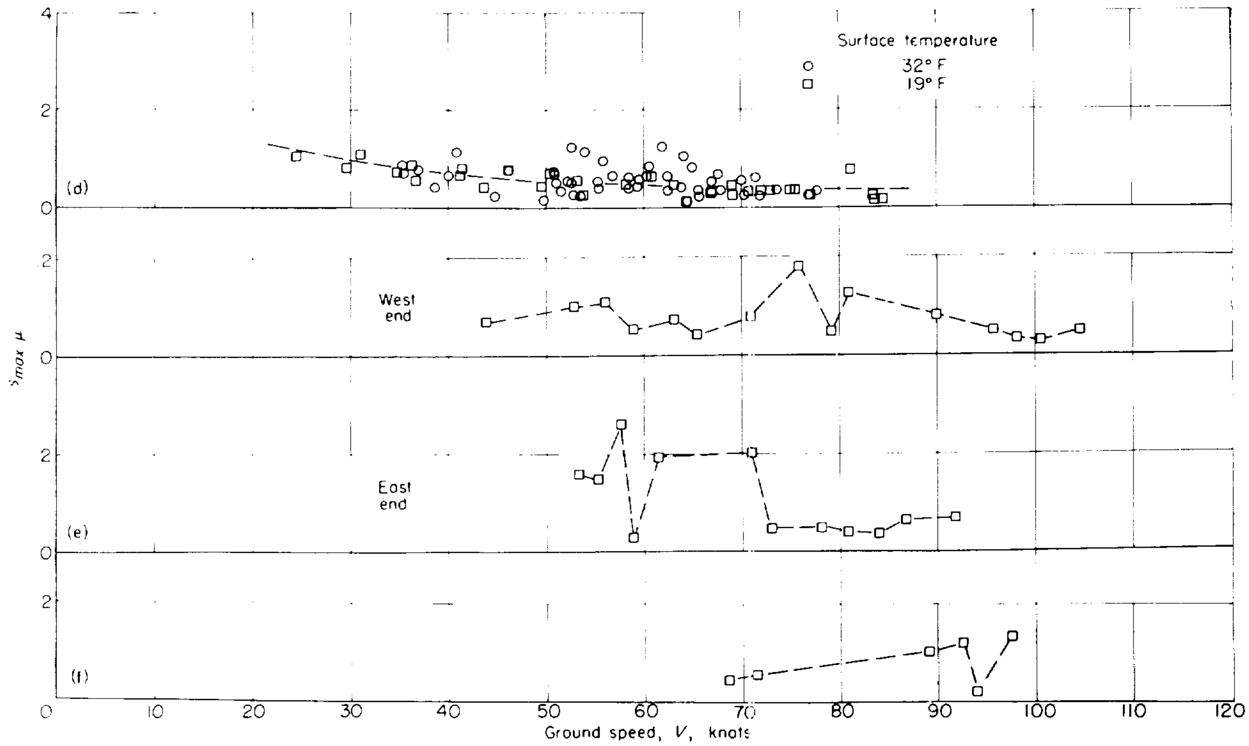

(d) Frozen lake surface (runway L).
(e) Wet portland-cement concrete (runway A). Right gear.
(f) Wet bituminous pavement (runway D); landing made during light rain shower. Right gear.

FIGURE 14.—Concluded.

progressed to lower speeds. The extremely low values of the friction coefficient at the higher speeds were ascribed, as before, to tire planing.

6. The mean values of wheel slip ratio at which the maximum friction coefficient was reached varied considerably with surface conditions and in some cases varied with speed.

LANGLEY RESEARCH CENTER,
NATIONAL AERONAUTICS AND SPACE ADMINISTRATION,
LANGLEY FIELD, VA., *January 23, 1959.*

REFERENCES

1. Milwitzky, Benjamin, Lindquist, Dean C., and Potter, Dexter M.: An Experimental Study of Applied Ground Loads in Landing. NACA Rep. 1248, 1955. (Supersedes NACA TN 3246.)
2. Potter, Dexter M.: An Experimental Investigation of the Effect of Wheel Prerotation on Landing-Gear Drag Loads. NACA TN 3250, 1954.
3. Batterson, Sidney A.: Recent Data on Tire Friction During Landing. NACA RM L57D19b, 1957.
4. Hall, Albert W., Sawyer, Richard H., and McKay, James M.: Study of Ground-Reaction Forces Measured During Landing Impacts of a Large Airplane. NACA TN 4247, 1958. (Supersedes NACA RM L55E12c.)
5. Allen, R. G., and Creech, W. T.: Tests for Determining the Coefficient of Friction of 44″ Smooth Contour Tires on Concrete Runways. MR No. MCREXA6-45257-4-1, Air Materiel Command, Eng. Div., U.S. Air Force, Feb. 27, 1948.
6. Giles, C. G., and Lander, F. T. W.: The Skid-Resisting Properties of Wet Surfaces at High Speeds: Exploratory Measurements With a Small Braking Force Trailer. Jour. R.A.S., vol. 60, no. 542, Feb. 1956, pp. 83-940.
7. Thompson, Thomas L.: Snow as It Affects Aircraft Ski Performance. WADC Tech. Rep. 53-154, U.S. Air Force, June 1953.
8. McConica, Thomas H., III: The Aircraft Ski. WADC Tech. Rep. 53-153, U.S. Air Force, July 1953.
9. Peters, R. W.: The NACA Combined Load Testing Machine. Proc. Soc. Exp. Stress Analysis, vol. XIII, no. 1, 1955, pp. 181-198.
10. Harrin, Eziaslav N.: Low Tire Friction and Cornering Forces on a Wet Surface. NACA TN 4406, 1958.
11. Hadekel, R.: The Mechanical Characteristics of Pneumatic Tyres—A Digest of Present Knowledge. S & T Memo. No. 10/52, British Ministry of Supply, TPA 3/TIB, Nov. 1952.

U.S. GOVERNMENT PRINTING OFFICE: 1960